CODEN:LUTEDX/(TEIE-5492)/1-77/(2023)

Industrial Electrical Engineering and Automation

Power system balancing in Swedish future scenarios of 2045 - Estimating contributions from V2G

Pontus Herrmann
Julia Jonasson

Division of Industrial Electrical Engineering and Automation
Faculty of Engineering, Lund University

Power system balancing in Swedish future scenarios of 2045 - Estimating contributions from V2G

Pontus Herrmann & Julia Jonasson

LTH
FACULTY OF ENGINEERING

Thesis for the degree of Master of Science
Thesis supervisors: Prof. Olof Samuelsson & Martin Lundberg
Examiner: Jörgen Svensson

Kommer elsystemet att kollapsa?

Populärvetenskaplig sammanfattning *Sol- och vindkraft kan inte kontrolleras, men byggs ändå ut i rasande takt, samtidigt som elen blir allt viktigare i samhället. Elsystemets nya utmaningar kräver nya lösningar för att fortsätta vara hållbart, säkert och kostnadseffektivt. I detta examensarbete utvecklas ett verktyg för simulering av elsystemet, och möjligheten att balansera elnätet med elbilar undersöks.*

Elsystemet kan liknas med en gammaldags slipsten, som måste snurra exakt 50 varv varje sekund. För att åstadkomma det måste den som vevar tillföra exakt lika mycket arbete som den som håller i kniven och bromsar stenen i bilden nedan. I elsystemet är vevaren alla kraftverk som trycker på, och konsumenterna är de som bromsar stenen genom att ta ut energi från systemet. Systemet är dock lite förlåtande, för även om vevaren trycker på lite mindre en kort stund, eller om sliparen bromsar lite extra ett ögonblick, så ändras inte rotationshastigheten så mycket eftersom att stenen som snurrar är så tung. På samma sätt har elsystemet stora generatorer som roterar lika snabbt som elen svänger. För att kniven ska slipas krävs balans i arbetet mellan de två personerna, och så även i elsystemet.

Hittills har vevaren i det svenska elsystemet sett till att trycka på precis lagom för att allt ska snurra i precis rätt hastighet, men hur gör man när man har mycket vindkraft, som snabbt ändras? En lösning är att konsumenterna anpassar sig till hur mycket energi som finns tillgänglig, alltså att man får anpassa slipningen till hur mycket som vevas, och detta brukar kallas efterfrågeflexibilitet.

Examensarbetet som vi presenterar i denna rapport grundar sig på scenarier om hur Sveriges elsystem kan se ut 2045, där vår elkonsumtion är dubbelt så stor som idag. Vi har skapat en modell av denna framtid för att möjliggöra för fler att utforska vilka problem som elsystemet kan stöta på. Ett känt problem att utforska är hur stora mängder elproduktion från sol och vind påverkar balansen i elsystemet. Det är svårt att veta hur mycket det ska blåsa och när solen kommer skina, vilket leder till stor oförutsägbarhet i när elen kommer att produceras och hur mycket. Vi har i examensarbetet undersökt vad denna oförutsägbarhet innebär för balansen i elsystemet, och därefter tittat på en lösning.

Lösningen är att utnyttja batterierna i elbilar som står uppkopplade till elnätet. Genom att skapa en modell av elbilsbatterier i Sverige har vi simulerat elsystem i obalans och studerat hur batterierna minskar obalanserna. Den tekniska potentialen visar sig vara väldigt stor.

Contents

Abstract

The ongoing climate change calls for an immediate decarbonization of society, where one important measure is a rapid transition of the energy system through an expansion of variable renewable energy sources, such as wind and solar photovoltaic power production. This transition imposes new challenges to the electrical power system, not least from a power balance perspective.

This master's thesis report consists of two parts, beginning with a tutorial on power system balancing. Starting from a theoretical approach, fundamentals of the power balance is presented, followed by a description of how this is realized in technology and on the markets for energy, balance and ancillary services. With the rapid transition of the energy system, it is of great interest to work with forward planning, and here this is done by using two electrification scenarios for year 2045 developed by Svenska kraftnät, the Swedish transmission system operator, in their long term market analysis. The second part consists of two quantitative studies, both based on raw data from Svenska kraftnät scenario simulations. In the first study, an electrical grid simulation tool is developed, using the further developed network model Nordic 46, the grid simulation software PowerFactory and a Python script. This is validated by examples and comparisons with Svenska kraftnät simulations, and may be used for further studies.

The second quantitative study focuses on power system balancing on a minute scale. This part is based on the work of a PhD project at the KTH Royal Institute of Technology, where production and consumption time series are interpolated based on their characteristics, and the need for balancing power is defined as the difference between consumption and production. A promising solution to abate this power imbalance is the use of bidirectional charging of electric vehicles, also known as vehicle to grid. A model of aggregated electric vehicles is built and used to investigate to what extent vehicle to grid can abate the power imbalance. Results indicate a great potential in the technology, but it relies on more intelligent battery control schemes as well as a market enabling it to be part of balancing the power system.

Preface

This master's thesis marks the end of the M.Sc. program in Engineering Physics and has been carried out at the division of Industrial Electrical Engineering and Automation (IEA) at the Faculty of Engineering (LTH), Lund University. The project has been done in association with the Swedish Electricity Storage and Balancing Center and also aims to be a contribution to the doctoral research project *Managing grid capacity with storage* within the centre.

We want to express our deepest gratitude to our supervisors Professor Olof Samuelsson and PhD student Martin Lundberg, for enlightening and valuable guidance during a sometimes confusing process. Chapters 3.1 and 5 have been written in close collaboration with our fellow students Simon Hessman and Frida Lundberg, and we want to thank them for well functioning and pleasant team work. We also want to thank Henrik Nordström (KTH), Emil Hillberg (RISE), Alexandra Nikoleris (LTH), Morten Hemmingsson (LTH) and all colleagues at the division of Industrial Electrical Engineering and Automation for helpful contributions, insights and delightful conversations in the lunch room.

This report and underlying work have been carried out equally between both authors.

Lund, June 1, 2023
Pontus Herrmann & Julia Jonasson

List of abbreviations

AC	Alternating Current
ACE	Area Control Error
AGC	Automatic Generation Control
AM	Autonomus Mobility
AOF	Activation Optimization Function
ATC	Available Transmission Capacity
BESS	Battery Energy Storage System
BZ	Bidding Zone
BZB	Bidding Zone Border
CA	Control Area
DC	Direct Current
EF	Elektrifiering Förnybart (Eng. Electrification Renewable)
ENTSO-E	European Network of Transmission System Operators for Electricity
EP	Elektrifiering Planerbart (Eng. Electrification Dispatchable)
EV	Electric Vehicle
FCR-N/D	Frequency Containment Reserve Normal/Disturbance
FFR	Fast Frequency Reserve
a/mFRR	automatic/manual Frequency Restoration Reserve
HVDC	High Voltage Direct Current
ISP	Imbalance Settlement Period
LMA	Long-term Market Analysis
N44	Nordic 44
N46	Nordic 46
NBM	Nordic Balancing Model
NTC	Net Transfer Capacity
PF	PowerFactory
PHEV	Plug-in Hybrid Electric Vehicle
PO	Privately Owned
PoN	Post Netting
PrN	Pre Netting
PV	Photovoltaic
QS	Quantitative Study
(v)RES	(variable) Renewable Energy Source
RE	Retailer
SMR	Small Modular Reactor
SoC	State of Charge
Svk	Svenska kraftnät
TP	Trading Period
TSO	Transmission System Operator
V2G	Vehicle to Grid

Chapter 1

Introduction

The current era of climate change and global warming entails great threats to society and mankind. One of the most important solutions to these problems is a general electrification of the society through a massive expansion of renewable electricity production while phasing out existing fossil energy infrastructure. In an energy context, this is a very rapid transition, and it imposes new challenges for the current electrical power system. A matter of interest in this area is power system balancing, meaning that electricity consumption and production are equal both momentarily and on a long term horizon.

This master's thesis starts from a technical point of view and investigates future power system balancing by using scenarios of a 2045 power system. A network model of the transmission system in the Nordic countries is developed and used for grid simulations, and energy balance is investigated on a minute scale, for which bidirectional charging of electric vehicles is studied as a plausible solution.

1.1 Purpose

Power system balancing might appear to be a complex and technical subject, and therefore this thesis aims to be an educational contribution to this area by investigating power system balance in a broad context. The approach for this is an explanatory, rather than concise, background and theoretical section, followed by two illustrative and quantitative studies with the idea to give different perspectives on the topic. By developing a simulation tool, this work paves the way for further studies including electrical grid simulations of the Nordic power system with a higher penetration of renewable power production. Another more concrete objective is to quantify the need for balancing power in year 2045 power system scenarios with high degree of electrification, and how an electrified vehicle fleet can contribute to the balancing.

At the same time, this master's thesis constitutes the end of the M.Sc. program in engineering physics. Therefore, an additional ambition for this project is to wrap up five years of university studies by using knowledge and tools gained in completed courses during this time.

1.2 Research questions

With the general purpose of being an educational report, the following scientific questions are used in the second quantitative study, where the need for balancing power is investigated together with possible solutions to the matter.

- What is the need for balancing power in different future scenarios with high share of varying renewable energy sources?
- What is the potential of bidirectional charging of electric vehicles to contribute to future power system balancing?

1.3 Limitations

The topic of power system stability and balance is both broad and deep. This thesis is focused on power and energy system balancing, and how this is implemented on the balancing market.

With a lot of possibilities and uncertainties when working with future scenarios, the work quickly grows out of hands if several scenarios are taken into account. In this context, only two scenarios are used, both relying on electrification. Further, both the quantitative studies are based on data produced by the Swedish transmission system operator Svenska kraftnät. This data leaves some questions and concerns, which are discussed in chapter 7, but in addition to that it is assumed to be reliable and conclusions are drawn based on it.

1.4 Structure of the report

Figure 1.1 shows a flow chart of the structure of the report, consisting of an educational overview of electric power system balancing, followed by two quantitative studies aiming to give deepened perspective on the main topic.

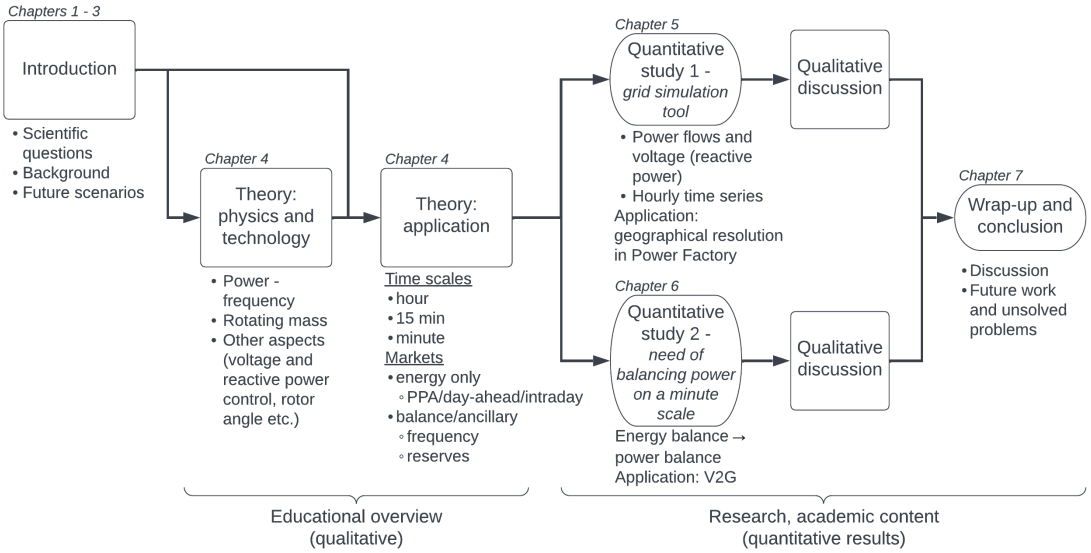

Figure 1.1: Schematic figure of the report structure.

In chapter 2, the reader is briefly introduced to the fundamental concepts of an electric power system in general, and characteristics regarding production, consumption and transmission in Sweden. The concept of scenarios is presented in chapter 3, followed by a more profound review of Svenska kraftnät's long term market analysis with associated data that is used in the quantitative studies.

Chapter 4 starts with a physical and technical foundation of electric power system balancing, where the instantaneous power balance and some other important concepts are derived. The technological concepts are expanded to a description of the Swedish market implementations, how energy is traded and structure of the balancing market. As there is a transition of the entire energy system and currently a large scepticism regarding the energy markets' performance, the final section of the chapter is dedicated to ongoing and upcoming changes of the electricity markets.

In the first quantitative study, chapter 5, a tool for network simulations is developed for future scenarios, consisting of a grid model and a Python script automating time series of load flow simulations. This is validated by data analysis and comparisons to another simulation. The second quantitative study, chapter 6, investigates the need for balancing power in 2045 by interpolating time series to higher time resolution based on data category and their respective characteristics. As a partial solution to the need for balancing power, bidirectional charging of electric vehicles, also known as vehicle to grid, is investigated in different automotive scenarios, through a model of aggregated vehicle batteries.

In the final chapter 7, the results, stated assumptions and interpretations are analyzed and discussed, and some suggestions of future work and model development are presented.

Chapter 2

Background

The most fundamental parts in a power system are the producers and consumers of electricity. If the production and consumption are located in different places, there is a need of power transmission to the consumers. The most common method for transferring electrical power in Europe is to use three-phase alternating current (AC), with a nominal frequency of 50 Hz, and with many different voltage levels. With an AC grid, several producers and consumers can be interconnected. They then form a *synchronous area*, which share the same frequency independent of voltage level and location. Traditionally the electric power comes from synchronous generators, directly connected to the grid. Their rotational velocity is reflected in the grid frequency, and they electromagnetically synchronize to the same common frequency. Production units with widely varying rotational speed or no moving parts are instead connected through power electronic components, that convert a direct current (DC) to AC, which usually is the case for wind and solar power. If there is a demand for electrical power transfer to another synchronous area, the common method is to use high voltage DC (HVDC) connections, where AC is first converted to DC, then transferred through a cable and finally reconverted to AC, with desired characteristics in the receiving end. [1]

This sections present the production, consumption and transmission of electricity in the Nordic synchronous area in 2023, with special focus on Sweden.

2.1 Production

Sweden has undergone several stages of electrification. At the first stage, the hydro power was developed, mainly in the 1940s-1960s. The second step was the construction of nuclear power, which took place in the 1970s and 1980s. The third step is the current expansion of varying renewable energy sources (vRES), mainly consisting of wind and solar power. In 2022, the hydro power produced around 80 TWh, nuclear power 50 TWh and wind power 33 TWh, corresponding to 40, 30 and 20 % of the Swedish electricity generation respectively [2]. The remaining electricity production consisted of 2 TWh from solar photovoltaic (PV) production and 15 TWh combined heat and power electricity generation. Historic trends can be seen in figure 2.1.

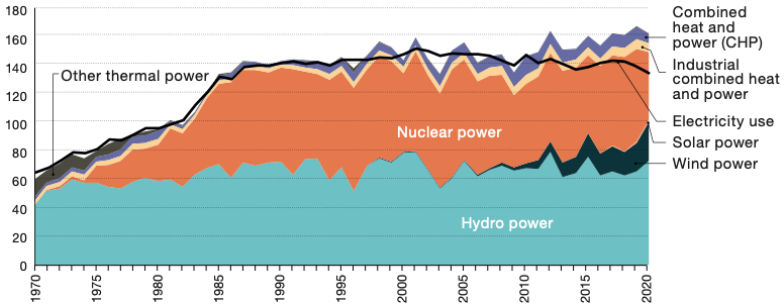

Figure 2.1: Electricity production categories in Sweden 1970-2020, in TWh [3].

2.2 Consumption

The Swedish consumption of electricity increased steadily until around 1990, and has been relatively constant since then. Even though new areas of consumption have arisen, e.g. digital systems and infrastructure, there has been a significant increase in energy efficiency through e.g. heat pumps replacing direct electric heating [4]. The consumption can be split into user categories as in figure 2.2.

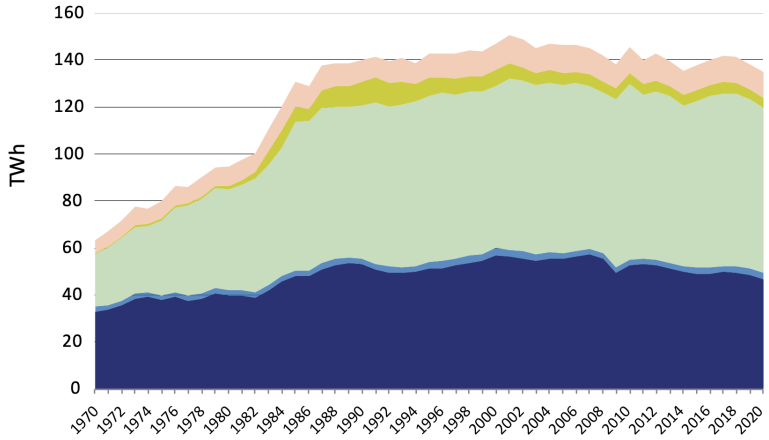

Figure 2.2: Electricity consumption categories in Sweden 1970-2020 [4]. Categories from below: Industry (dark blue), Transports (light blue), Residential and Services (light green), District heating and Refineries (yellow-green) and transmission losses (pink).

In Sweden and the Nordic countries there are temporal consumption patterns on seasonal, weekly and daily basis. This is due to significant seasonal variation in temperature and daylight, working days and hours. Examples of consumption can be seen in figure 2.3a and 2.3b.

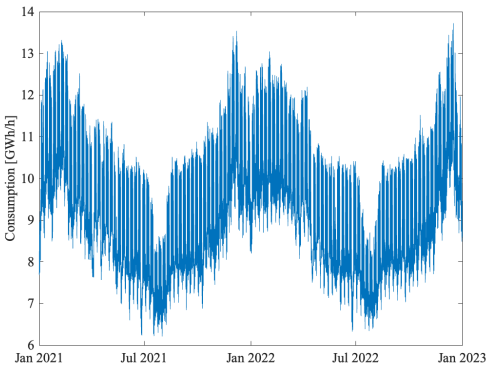

(a) Hourly values of total electricity consumption in Sweden demonstrating seasonal variations. Note the holiday period in July.

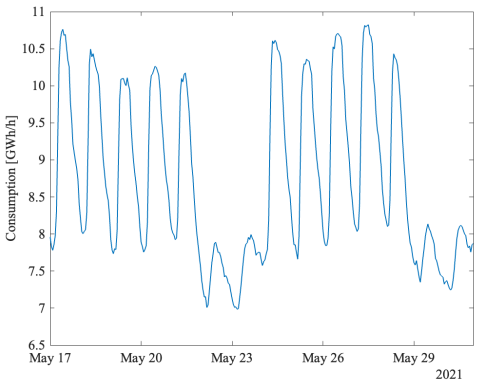

(b) Detail of figure 2.3a, showing weekly and daily consumption pattern in Sweden, Monday, May 17 - Sunday, May 31, 2021. Note the smaller consumption on weekends.

Figure 2.3: Example of seasonal, weekly and daily consumption patterns in Sweden [5].

2.3 Transmission and market

With a lot of hydro and wind power production in northern Sweden and most of the consumption in the more densely populated southern Sweden, there is a natural need for long distance transmission. This is handled with high voltages of 230-400 kV in the transmission grid, which is owned and operated by the Swedish Transmission System Operator (TSO) Svenska kraftnät (Svk) [6]. After being transferred long distances, the power is transformed to lower voltages (40-130 kV) and sent out on a distribution grid, to which large consumers are connected. Small and medium-sized consumers use even lower voltages (0.4-40 kV), which is distributed on local distribution networks.

All power transmission uses power lines, often overhead but sometimes underground cables, which have rated current and voltage, and thus a limited power transfer capacity. An important term here is the time varying Net Transfer Capacity (NTC), which is the physical capacity with a transmission reliability margin for unforeseen events subtracted, and is what is used on the electricity market. In some locations the limitations become problematic, forming transfer bottlenecks. When trading electricity these bottlenecks have significant impact on the market, giving geographical constraints for sellers and buyers. In Sweden and Norway this has been handled by introducing bidding zones (BZs) where electricity can be traded without these constraints to an equal price within the area, while at the same time causing price differences over bidding zone borders (BZBs) [6]. Interconnections between countries are natural bottlenecks, resulting in BZBs between them. In the Nordic synchronous area there are four BZs in Sweden, five in Norway, one in Finland and one in eastern Denmark, which can be seen in figure 2.4. Also seen in the figure are the Baltic countries and western Denmark, which is part of to the Continental Europe synchronous area, and is connected to the Nordic area through HVDC interconnections.

Figure 2.4: BZs in the Nordic synchronous area and current transfer capacities between them [7].

Chapter 3

Looking into the future

In order to handle future challenges arising from the decarbonization of society, such as electrification of heavy industry and transportation, and a higher share of intermittent power production, the power grid will have to adapt. This adaptation might come both as an expansion of the transmission system, but also as a reinforcement of the existing structure. Current plans for changes in the transmission system in Sweden are presented in the *System Development Plan* issued by Svk [8]. The latest version of this plan consists of undertakings for the time period 2021 to 2031. The base for these plans are the short- and long-term market scenarios published by Svk in two separate reports named *Kortsiktig marknadsanalys* (KMA) and *Långsiktig marknadsanalys* (LMA) respectively [9, 10]. The KMA report is published every year, the latest being KMA 2022 which looks at the horizon of 2027, while the LMA report is published every second year, the latest being LMA 2021 which looks at the horizon of 2045. One thing often presented as a key in future scenarios, for handling the future challenges in the power system, is flexibility. In this report, flexibility is defined as the flexible use of energy in both volume and time. In case an electricity user can store energy and inject the electricity back to the grid, this is also included in the definition.

3.1 General about scenarios

Scenarios are made-up versions of the future that can be either probable, possible or desirable. They can be used both as a way of making predictions of the future, but also as a tool to broaden the possibilities which are considered, i.e. serve as a planning tool [11]. Some scenarios might not be desirable at all, but rather present guidelines for what directions of development that should be avoided.

Svk uses scenarios to identify future problems and needs in the power grid [10]. Their scenarios pose as different possible development paths for the grid, where each path comes with its own challenges and opportunities. Thus, the scenarios presented in the Svk LMA are not forecasts of the future, but tools which are used to take measures to counter future challenges that may occur in the grid [10]. Therefore none of the scenarios presented by Svk will be a perfect description of the future.

Scenario planning is carried out globally, and in Europe, all TSOs cooperate to produce base data and reports for both national and international scenarios. In the scenarios from Svk, the

assumptions made regarding development in continental Europe and Great Britain are based on the scenarios in the Ten-Year Network Development Plan (TYNDP 2020) developed by the European Network of Transmission System Operators for Electricity and Gas (ENTSO-E and ENTSOG). Assumptions on the Swedish development presented in LMA 2021 are then used as input for the next TYNDP 2022. The results are thus closely anchored to the work done by all the European TSOs. Work with scenarios is also performed within the industry and it can be of interest to compare assumptions, inputs and results from these. In Sweden, the most extensive work beyond Svk's LMA is published by the major employers' organization for private sector and business sector companies in Sweden, Svenskt Näringsliv [12].

The main difference between the analysis performed by Svenskt Näringsliv and the one by Svk is the type of optimization method used. Svk has, based on assumptions, proposed input data and from an optimization of operation gained information about how the system is best operated in each scenario and which challenges there are. Svenskt Näringsliv on the other hand has performed an optimization of the whole system, which results in a suggestion on how to design the system to the lowest possible system cost. The scenarios from Svenskt Näringsliv and Svk are in many aspects comparable. Assumptions and identified trends are mainly the same, with an increased demand from transport and industry, and in particular the steel industry.

3.2 Svk scenarios in LMA 2021

Four scenarios are presented in the long-term market analysis, two of them being of interest for the purpose of this thesis: Elektrifiering förnybart (EF) and Elektrifiering planerbart (EP), translated to Electrification renewable and Electrification dispatchable respectively. They both assume a large increase in electricity demand of 300 TWh until the year 2045, but the demand is met by different power production portfolios. Both are driven by net zero emissions of CO_2 and a large expansion of green industry, especially in the north of Sweden. One example of these new industries is HYBRIT, which will produce fossil free steel by replacing coal and coke with hydrogen [10]. The integration between electricity production and the use of hydrogen will be extensive in both scenarios, but its flexibility services will be of higher importance in scenario EF [10].

The electricity-intensive industry is assumed to follow approximately the same load profile as today. However it is also assumed that a certain level of flexibility exists. This flexibility occurs due to a price-sensitivity where a part of the industry reduces its production or switches to another energy carrier than electricity at prices between 100-120 euros per MWh. When the price exceeds 200-500 euros per MWh some of the industries are assumed to shut down [10].

In scenario EF, the Swedish nuclear power plants are taken out of service after a lifetime of 60 years, which means that the Swedish goal of a completely renewable electricity system year 2045 is reached. Offshore wind power expands around all of Sweden, and land based wind power is built mostly in the northern parts of the country. Solar power is built mostly in cities together with batteries. However, the large portion of wind and solar power in the power system means that only 22% of the installed capacity is dispatchable. Thermal power production will still be used, but decrease somewhat, due to the fact that re-investments are not profitable. To compensate for this more residual heat will be used [10].

The expansion of solar and wind power is large in scenario EP as well, however not as extensive as in scenario EF. This has to do with the fact that scenario EP also utilizes nuclear power. Other thermal power production will vary somewhat until 2045, but remain approximately the same as it is today. All together the renewable electricity production make up 89% of the installed capacity in 2045 [10]. The inclusion of nuclear power entails a share of dispatchable electricity production of 40% in 2045. This, together with local dispatchable power production in cities, results in few hours per year with issues concerning the energy balance. A higher share of dispatchable power production also results in very little power being wasted due to a too excessive power generation [10].

The general power system challenges appear mainly in scenario EF. In the scenario, there will be hours when the electricity generation fails to meet the electricity demand and hours when the electricity generation is too high to handle without disconnecting or curtailing generation. Due to nuclear power plants taken out of service and a higher share of wind and solar power, the system inertia, further explained in section 4.1, will be lower than today in scenario EF, which poses a threat to the grid frequency stability [10]. The basis for this particular challenge will be discussed further in chapter 4.

As for scenario EP, the overall balance in the system is improved compared to today, partly due to the increased electricity consumption in the north of Sweden and the increased power production in the south. There is also a better geographical balance between cities and rural areas, since dispatchable power production is likely to be installed in urban regions. However, the large increase in electricity consumption in SE1, largely due to the electrification of the industry, will cause a shortage of energy there and thus also higher prices compared to the rest of Sweden [10].

3.3 Description of data

The data on which the quantitative studies in chapters 5 and 6 are based is the simulation results from Svk's LMA [13], scenarios EF and EP for year 2045. The raw data consists of time series with hourly resolution divided into the following components:

- consumption,
- hydro power production,
- load curtailment,
- nuclear power production,
- other thermal power production,
- vRES power production,
- AC and HVDC flows on BZBs,
- vRES curtailment,
- and BZ prices.

The time series are based on simulations using 35 different weather years, resulting in 305 760 hours of data for each component. The weather years are years of actual weather measurements spanning from 1986 to 2021. Thus, when referring to one of these years, it is the future scenario of 2045 based on weather data from the historic year that is actually referred to.

Flexibility is handled differently in the data depending on the origin of the flexibility service. In both scenario EF and EP, some degree of flexibility is assumed from hydrogen production, industry, charging of electric vehicles (EVs) and local battery energy storage systems (BESSs) in households. Flexibility from bidirectional charging of EVs, also known as vehicle to grid (V2G), is not included. The degree of flexibility is limited to smart charging, i.e. prioritizing charging at times of low demand. The V2G solution will be further studied in chapter 6. Flexibility from electricity-intensive industry has already been mentioned in section 3.2, and consists of reduced power demand when the electricity price reaches certain levels. This flexibility has its own component, named previously as load curtailment. The flexibility from hydrogen production and EV charging are both included in the component consumption, making it hard to distinguish between individual patterns. If correctly balanced, these terms can be written as an equality (3.1),

$$\begin{aligned}\text{Hydro} + \text{Nuclear} + \text{Other thermal} + \text{Offshore} + \text{Onshore} + \text{Solar} + \\ + \text{Export}_{\text{net}} + \text{Load curtail} = \text{vRES Curtail} + \text{Consumption},\end{aligned} \tag{3.1}$$

but this is not the case with the data. If instead writing the balance as in (3.2) and forming a residual, a relatively periodic residual pattern with some outliers appears as in figure 3.1a. The periodicity can be explained by aggregated household BESS flexibility, and is thus not included in any component nor has its own. Similar patterns appear in the Swedish bidding zones, while NO1, NO3, NO4 and FI have close to 0 residuals, and NO2, NO5 and DK2 have perplexing, unexpected residuals, of which can be seen an example in figure 3.1b.

$$\begin{aligned}\text{Hydro} + \text{Nuclear} + \text{Other thermal} + \text{Offshore} + \text{Onshore} + \text{Solar} + \\ + \text{Export}_{\text{net}} + \text{Load curtail} - \text{vRES Curtail} - \text{Consumption} = \text{Residual}\end{aligned} \tag{3.2}$$

The vRES component includes both wind and solar power production. In order to properly see the effect of different renewable energy sources it is desired to handle these separately. A method for dividing the aggregated vRES data developed by Henrik Nordström is used [14]. The script utilizes data on installed capacity and load factors for each hour for the different renewables to split the vRES data proportionally according to equation 3.3. Load factors, LF_{type}, are obtained from the Pan-European Climate Database [15]. The share of total installed capacity, $\text{share}_{\text{type}}$, is calculated from capacities for the year of interest obtained from the LMA and Nordic Grid Development Perspective [16]. The script results in three new components (onshore and offshore wind power production and solar PV power production), which replace the vRES component.

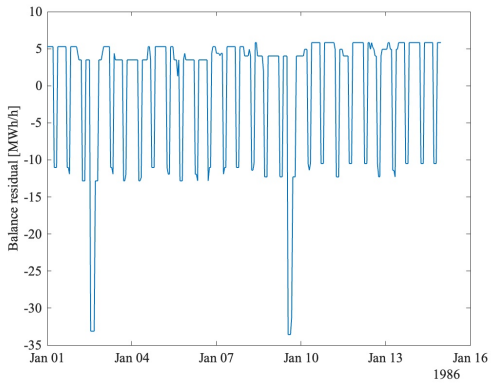

(a) Example of periodic, zero-mean balance residual (3.2) in BZ SE2, January 1-15, weather year 1986.

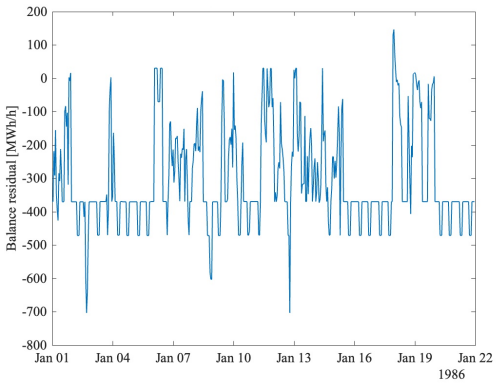

(b) Example of stochastically varying, non-zero-mean balance residual (3.2) in BZ DK2, January 1-21, weather year 1986.

Figure 3.1: Example of balance residuals [13]. Note the difference in magnitude.

$$\begin{aligned}\text{Energy share}_{\text{type}} &= \\ &= \text{vRES} \cdot \frac{\text{LF}_{\text{type}} \cdot \text{share}_{\text{type}}}{\text{LF}_{\text{PV}} \cdot \text{share}_{\text{PV}} + \text{LF}_{\text{offshore}} \cdot \text{share}_{\text{offshore}} + \text{LF}_{\text{onshore}} \cdot \text{share}_{\text{onshore}}}\end{aligned} \tag{3.3}$$

Some illustrating examples of simulated consumption, hydro and vRES production for scenarios EP and EF can be found in figure 3.2 for the Nordic synchronous area as well as for Sweden. Similar patterns can be seen when comparing different scenarios, indicating that the same weather data has been used in all simulations. In Sweden the vRES power production alone exceeds the consumption, especially in the EF scenario in figure 3.2d, but this production can be exported to other Nordic countries. In these figures it can also be seen that when there is very little vRES production, hydro power production increases to maintain the energy balance. The consumption in figure 3.2 can be compared to figure 2.3, indicating a much less periodic pattern in the future scenarios. Also the hydro power production is worth noting in figures 3.2c and 3.2d, which has a constant dispatch for several days. This will be further discussed in section 7.1.

Another illustrative example of the simulated time series can be seen in figure 3.3, where the residual load, defined as consumption minus vRES production, are plotted for the Nordic synchronous area and Sweden for both scenarios EP and EF. It is clear that the residual load in scenario EF varies significantly more than in EP. The residual load is what dispatchable production, flexibility and export have to take care of, and both the sizes and variability makes this a challenging task to handle. Especially in Sweden the residual load sometimes is negative in the EF scenario, meaning that the vRES production is higher than consumption demands. This is compensated for with export and curtailment in this case, since demand flexibility is already included in the consumption data.

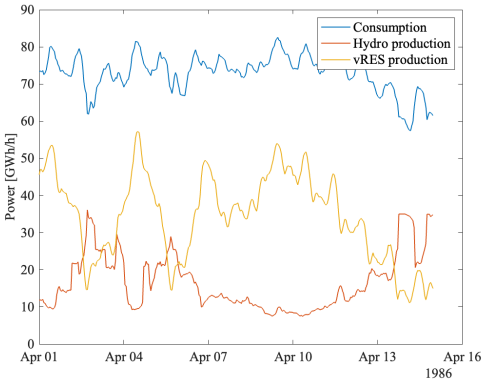

(a) Consumption, hydro and vRES production in Nordic synchronous area, scenario EP.

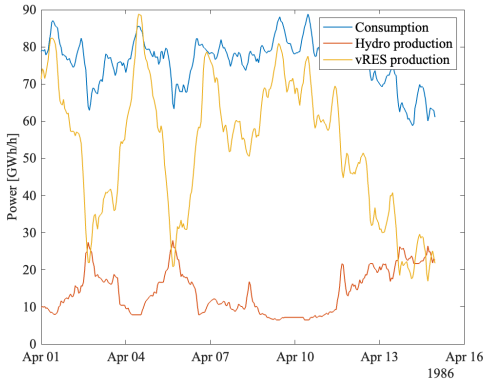

(b) Consumption, hydro and vRES production in Nordic synchronous area, scenario EF.

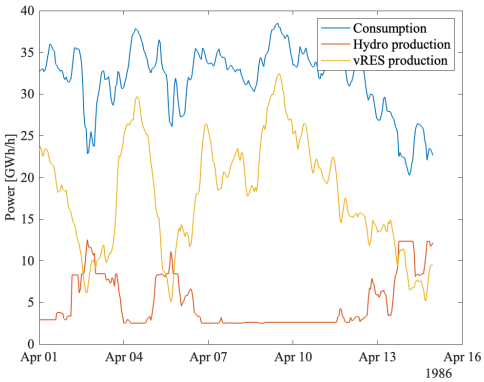

(c) Consumption, hydro and vRES production in Sweden, scenario EP.

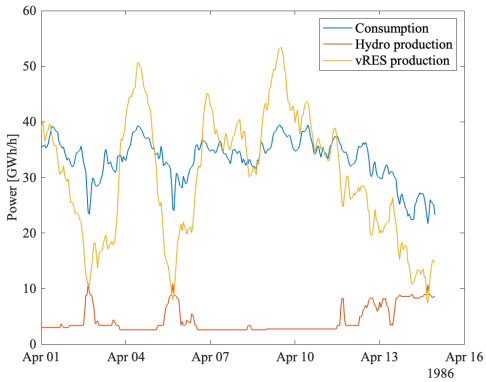

(d) Consumption, hydro and vRES production in Sweden, scenario EF.

Figure 3.2: Simulated examples of consumption, hydro power production and vRES power production for 2 weeks in April, weather year 1986 [13].

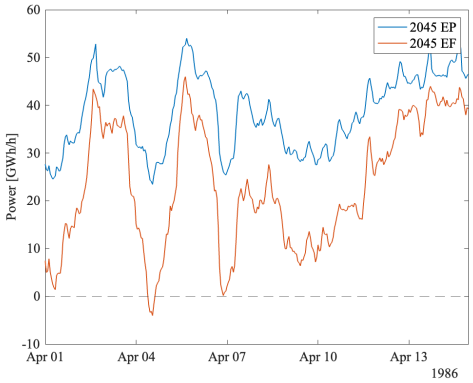

(a) Residual loads in Nordic synchronous area.

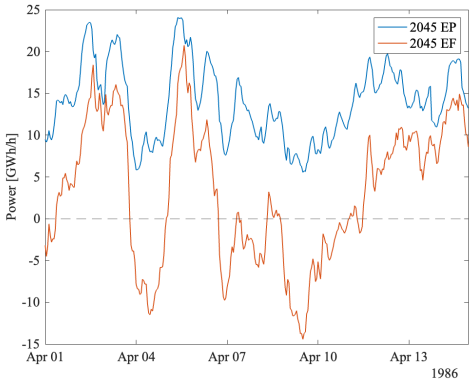

(b) Residual loads in Sweden.

Figure 3.3: Residual load, i.e. consumption - vRES production, for EP and EF scenarios [13].

Chapter 4

Power system balancing

With the main purpose of this thesis to study future imbalances in the Swedish power system, it is of utmost importance to first have an understanding of what power system balancing entails. The previous chapter paints a picture of the current and two possible future power systems, but omits the premises on which they function. The following sections in this chapter deals with these premises, first from a physical and technological perspective, followed by a market perspective.

The technical sections 4.1-4.2.1 are to high extent based on [1], which serves as reference in this part if nothing else is indicated.

4.1 Fundamentals

As mentioned in chapter 2, most of the power generating units and some of the consuming units are synchronously connected to the grid, meaning they have a rotational frequency directly proportional to the actual grid frequency f, and that the electrical frequency is directly linked to a mechanical quantity. This is closely related to Newton's second law on rotational form (4.1), where J, ω_m and T represents the moment of inertia, mechanical angular velocity and torque respectively.

$$J\frac{d\omega_m}{dt} = \sum T \tag{4.1}$$

For a synchronous power system, the moments of inertia of the synchronous rotating units can be summarized to a corresponding system moment of inertia. Similarly, the resulting mechanical torques of the generators can be summed up to a driving mechanical torque T_m, and the loads are represented by a braking electrical torque T_e. Equation (4.1) can now be rewritten in the so called swing equation form (4.2), where $\omega_{el} = 2\pi f$, and f is the electrical frequency.

$$J_{sys}\frac{d\omega_{el}}{dt} = T_m - T_e \tag{4.2}$$

Replacing $T = P/\omega \sim P$, where P denotes power, it can be seen that a positive net power leads to a frequency increase and vice versa, and the acceleration is proportional to the sum of the moments of inertia connected to the grid. The swing equation (4.2) can further be rewritten as (4.3), forming the inertia constant H with unit Ws. This is the energy stored in the rotating masses synchronously connected to the grid, and this energy storage is charged and discharged by the unbalance between generation and consumption throughout the synchronous area. H is

sometimes normalized with respect to the generators' nominal power, with the normalized unit seconds, and is then suitable for comparisons independent of generator size. An example of how the frequency varies over the day can be seen in figure 4.1a. From equation (4.3), H might appear as constant over time, but as can be seen in figure 4.1b the inertia constant varies over the day, depending on the size and number of generators that are synchronized to the grid.

$$\frac{2}{\omega_{m,s}} \frac{J\omega_{m,s}^2}{2} \frac{d\omega_{m,s}}{dt} = \frac{2H}{\omega_{m,s}} \frac{d\omega_{m,s}}{dt} = \frac{4\pi H}{\omega_{m,s}} \frac{df}{dt} = P_m - P_e \tag{4.3}$$

In order for the connected components to function well, it is necessary to maintain the frequency very close to the nominal value of $f_{nom} = 50$ Hz, and therefore an important key value for power quality is the frequency deviation $\Delta f = f - f_{nom}$. To fulfill the fundamental goal of satisfying the demand, the power production must equal the consumption. According to the swing equation (4.2), a negative power balance leads to a decreasing frequency, which is equal and measurable in the whole synchronous system. This way a system power deficit can be known and thus compensated for by increasing power production, which will be further described in section 4.2. The inertia J allows a small, temporary imbalance before compensating. If a fault occurs, the power system can "borrow" a little energy from the rotating masses by slightly changing their rotational frequency while ramping up the driving power and thus the mechanical torque. However, over time the net power deviation has to be non existing.

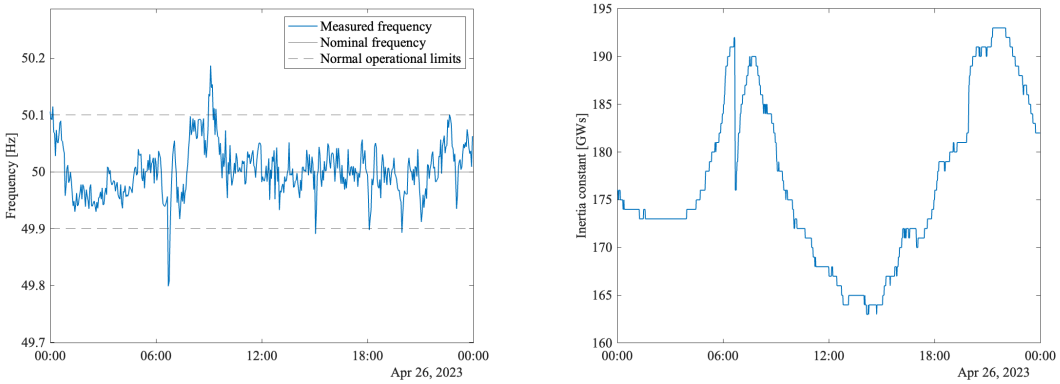

(a) Measured frequency, with 3 minute resolution, in the Nordic synchronous area. The frequency is close to nominal except for the dip at 06:40.

(b) Inertia constant H as defined in (4.3) in the Nordic synchronous system. The variations are normal except for the dip at 06:40.

Figure 4.1: Measured frequency and inertia in the Nordic synchronous system. At 06:40 two nuclear power units, delivering 2130 MW in total, were disconnected due to a frequency and voltage deviation also seen in figure 4.5, which can be seen in the quick decrease of both the frequency and inertia constant at that time. [17]

Modern power production with highly variable rotational speeds or without moving parts, typically wind or solar PV power plants, cannot be synchronously connected to the grid. The most common solution is to use a power electronic inverter, which creates sinusoidal waveforms with the frequency f of the grid, allowing the power to be injected. Modern inverters are to high extent controllable in terms of voltage, power angle and waveform characteristics, but must always satisfy the balance power input equals power output plus internal losses. A high share of non-synchronous vRES power production thus implies a correspondingly low amount of synchronized rotating mass, making the power system more sensitive to disturbances and component failures.

A sometimes used analogy to get a better understanding of the power balance is a grind stone. Here, the driving torque corresponding to T_m or P_m is applied by the person driving the crankshaft, and the electric braking torque T_e or P_e is represented by the friction at the grindstone itself. When $T_e = T_m$ the grind stone continues in steady state rotation, but if the cranker stops, the rotation instantaneously starts slowing down. If the grindstone is large and heavy, the rotation is maintained for a longer time since the moment of inertia is large.

4.2 The reality of power system balancing

Given the exposition on the concept of balancing based on the fundamental physics, a matter of further explanation is how the balancing of the power system works in practice. To do so, the technical solution is presented, followed by the techno-economical market implementation with relevant actors.

The whole energy system is currently undergoing an enormous transformation due to decarbonization and the transition towards renewables. The transformation also includes the markets, and this thesis is being conducted right in the middle of this transformation. To bring order in these rapid changes, section 4.2 focuses on the present situation, and in section 4.3 upcoming plans and trends are presented. The transformation is global, and even though the perspective is meant to be Swedish it is natural to briefly broaden it when solutions align with the rest of the Nordics, Europe or the world.

Before digging into the details of balancing, it should be mentioned that a balanced system requires stability in terms of i.a. voltage and rotor angle, and also should be robust to technical failures. The nominal voltage is maintained by injecting or drawing reactive power in synchronous generators or shunt reactances and capacitors, and will be further investigated in chapter 5. In order to have a robust power system, the $N-1$ criterion is used, meaning that the intact system can handle sudden loss of any single component without delivery interruption. Within 15 minutes, the system should be N-1 secure again.

4.2.1 From a technical point of view

As the system frequency f is global and the change of frequency indicates a system power imbalance, the generator frequency is an appropriate measurement signal for control the mechanical power output. When, in steady state, there is a frequency deviation Δf, the desired generator power output change ΔP_m can be formulated as (4.4)

$$\Delta P_m = -\frac{\Delta f}{R}, \tag{4.4}$$

where R is the so called speed droop, also known as regulation constant, measured in Hz/MW. In an interconnected power system, several generators contribute to the regulating power as in (4.5).

$$\Delta P_{m,sys} = \Delta P_{m,1} + \Delta P_{m,2} + \Delta P_{m,3} + ... = -\left(\frac{1}{R_1} + \frac{1}{R_2} + \frac{1}{R_3} + ...\right)\Delta f = -\frac{1}{R_{sys}}\Delta f \tag{4.5}$$

To maintain stable frequency and adequate primary frequency control, the minimal area frequency response characteristic for the Nordic synchronous area is set to be $\frac{1}{R_{sys}} \geq 6000$ MW/Hz. Using equal regulation constant R for all generating units would make them contribute with the same amount of power, which would quickly saturate small units. To overcome this problem, the speed droop is normalized with the generator's rated power and electric frequency to a per unit (p.u.) unit, so that each generator contributes proportional to its size. This droop control corresponds to a proportional controller, and a power imbalance, ΔP_e, thus gives a stationary error (4.6) if a load change occurs.

$$f = f_{nom} - R\Delta P_e \tag{4.6}$$

It is of high interest to maintain the frequency as close to its nominal value as possible, and sometimes the primary control resources are close to saturating and need to be released. Therefore, a secondary control is added. The concept of this is to change the base generation set point, i.e., the generation at nominal frequency, and in automatic control terms this corresponds to an integrating controller. This can be done for generators both participating and not participating in the primary control. Previously the secondary control was done on manual basis, but has been automated in the Nordic system with the Automatic Generation Control (AGC) system since 2013 [18]. The secondary control (or load-frequency control) is activated when the frequency deviates from the nominal value and has two objectives: (1) reset the system frequency to its nominal value, and (2) have each control area (CA) maintain the transmission line interconnection (or tie-line) power flow at its scheduled value. Defining the Area Control Error (ACE) as in equation (4.7), i.e. the power imbalance in the CA minus its contribution to primary control, where Δp_{tie} is the difference between the actual and scheduled power flow from one CA to another, f is the system frequency and B_f [MW/Hz] is the frequency bias factor, the two objectives are equivalent to strive for ACE = 0. The second term represents the CAs contribution to primary control if $B_f = \frac{1}{R_{CA}}$.

$$\begin{aligned} \text{ACE} &= (p_{tie} - p_{tie,sched}) + B_f(f - f_{nom}) \\ &= \Delta p_{tie} + B_f \Delta f \end{aligned} \tag{4.7}$$

Over time, this desired behavior will be obtained by giving the secondary control the characteristics of an proportional-integral (PI) controller, expressed in equation (4.8) [19]. For each CA, the change in base generation set point, $\Delta p_{ref,i}$, for the units i, participating in the secondary control is proportional to the ACE with constant gain K_i, and the integral of the ACE. T_i is the integration time constant. If the power flow from the CA, p_{tie}, or the frequency f, is low, the ACE becomes negative and power generation in the CA should increase, hence the minus signs. The request to activate the reserve providing secondary control is dispatched at time intervals of 10 seconds [20].

$$\Delta p_{ref,i} = -K_i \cdot \text{ACE}_{CA} - \frac{1}{T_i} \int \text{ACE}_{CA}\, dt \tag{4.8}$$

Previously, the whole Nordic synchronous area constituted one CA. Thus, the secondary control was centralized and only relied on the system frequency deviation Δf in the ACE, (4.7), meaning the load changes in e.g. Norway could be absorbed by Finland. At the end of 2022, the Nordic

TSOs launched a new model for secondary control, with a new Activation Optimization Function (AOF) being the core, which takes both price and available transfer capacity into consideration [20, 21]. In the new model, each BZ is also an assigned CA.

The secondary control is primarily based on economics and agreements, rather than nominal size. In case of additional needs, a tertiary control is activated, with manual adjustments of generation power set points.

4.2.2 Markets

When dealing with energy system matters in a longer time perspective, it gets complicated to address the instantaneous power balance over long periods. Instead, the approach is to consider energy volumes during trading periods (TPs). The principle is to settle an energy balance for each TP through the futures, day-ahead and intraday markets, with higher accuracy closer to the delivery. As described in section 4.1, the power generation and consumption have to be balanced at every moment and the system has to be capable of handling disturbances and component failures. To ensure this, balancing resources are needed to address imbalances that arise in real time, and these are procured on the balancing market through different products.

The outline of this subsection is a brief explanation of the energy markets, followed by a more thorough overview of the balancing market, with description of working principles and relevant actors. The ancillary services market is also briefly explained. The general market structure can be seen in figure 4.2.

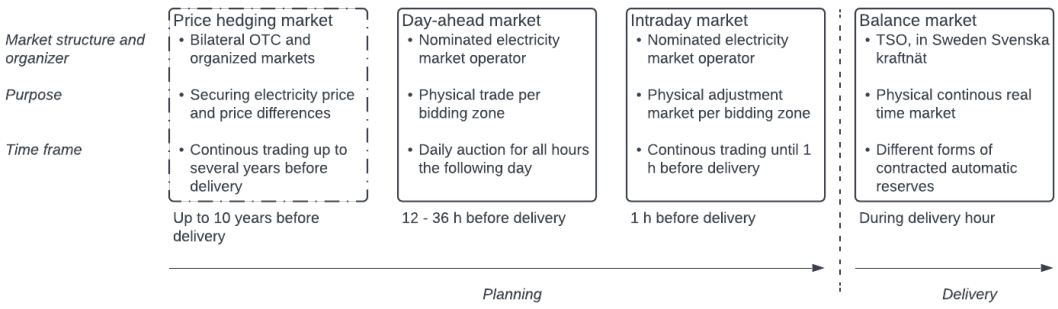

Figure 4.2: General electricity market structure divided by market type, presented along a timeline. Market structure and organizer, purpose and time frame is presented for each market.

Energy markets

The energy market with the longest time perspective is the so called *futures market*, where energy is traded with periods up to 10 years. Here the contracts can be physical, meaning that a producer should deliver the energy to the user (normally via the grid), or financial (also known as virtual or synthetic), which are used mainly for financial purposes [22]. The contracts are negotiated bilaterally between producer and consumer, and sometimes involves a balancing agent or a financial partner such as a bank. Financial futures contracts are also traded on Stockholm Stock Exchange, also called Nasdaq OMX [23]. One of the main purposes of the futures market is to secure the finances for building new production facilities, and these power purchase agreements

(PPAs) are crucial for the expansion of especially wind and solar power, where they lower the risk for both producer and financier [24]. At the same time the buyers, which often are retailers (REs) or industries with a high consumption, can guarantee the origin of the electricity, which is important for marketing and corporate social responsibility matters. The futures market is relatively unregulated due to its bilateral nature, but the most used contract standard in Europe has been developed by European Federation of Energy Traders. An extensive report about the futures market and PPAs can be found in [24].

Very little is known about exact production possibilities and consumption demands on the time scale of the futures market, and the vRES power producers' balancing agents must be able to provide the contracted power in times of low renewable power production [22]. This is one of the purposes of the *day-ahead market*, also known as spot market. In northern Europe, this market is mainly organized and operated by Nord Pool, but there is also another nominal electricity market operator called EPEX. The principle of this wholesale market is harmonized in Europe through the Euphemia algorithm[1], where all producers, REs and big consumers submit bids for buying or selling energy for each TP to the operator no later than noon one day ahead of delivery [26]. Then the market operator organizes the offers and buyers' bids from high to low and vice versa, and with respect to transmission capacities and technical conditions determine price crosses for each bidding zone, yielding production, consumption, HVDC export and indirectly net flows over BZBs. On the day-ahead market, marginal pricing is used, meaning the same price for all consumers and producers whose bids were accepted.

The third energy market is the *intraday market*. This opens at 14:00 the day before and closes 1 h before associated delivery TP. Unlike the day-ahead market, the intraday market uses pay-as-bid pricing, meaning that when there is an overlap, bids and offers can be accepted immediately on a continuous trading platform [22]. The actors are in general the same as on the day-ahead market, and the purpose here is mainly to compensate for adjusted forecasts or component failures.

Balancing market

On the balancing market, consumers and production units both can offer the TSO services that can be utilized for ensuring power balance in the ways explained in section 4.2.1. The products on the balancing market are categorized into primary, secondary and tertiary control, as can be seen in figure 4.3. Primary frequency control consists of frequency containment reserves (FCR), which in turn can be divided into FCR-N, FCR-D (up) and FCR-D (down) with respect to operating conditions (Normal and Disturbance). Secondary and tertiary frequency control consist of automatic and manual frequency restoration reserves (aFRR and mFRR) respectively.

[1]The Euphemia algorithm determines prices for all BZs and flows over BZBs in 25 European countries, with respect to available transfer capacities and technical constraints in power plants. [25]

	Primary control			Secondary control	Tertiary control
FFR	**FCR-N**	**FCR-D (up)**	**FCR-D (down)**	**aFRR**	**mFRR**
Fast frequency reserve	Frequency containment reserve Normal	Frequency containment reserve Disturbance Up	Frequency containment reserve Disturbance Down	Frequency restoration reserve Automatic	Frequency restoration reserve Manual
Activation	**Activation**	**Activation**	**Activation**	**Activation**	**Activation**
Automatic at 3 levels of deviation: 49.5, 49.6, 49.7 Hz	Automatic, linear in the interval 49.9-50.1 Hz	Automatic, linear in the interval 49.5-49.9 Hz	Automatic, linear in the interval 50.1-50.5 Hz	Automatic at deviations from 50 Hz	Manual at request from TSO
Activation time	**Activation time**	**Activation time**	**Activation time**	**Activation time**	**Activation time**
100% within 0.7 s (49.5 Hz) 1.0 s (49.6 Hz) 1.3 s (49.7 Hz)	63% within 60 s 100% within 3 min	50% within 5 s 100% within 30 s	50% within 5 s 100% within 30 s	100% within 5 min	100% within 15 minutes
Vol. requirements (Sweden)	**Vol. requirements (Sweden)**	**Vol. requirements (Sweden)**	**Vol. requirements (Sweden)**	**Vol. requirements (Sweden)**	**Vol. requirements (Sweden)**
Up to 100 MW	231 MW	Up to 558 MW	Up to 538 MW	Up to 111 MW	No requirements

Figure 4.3: The products available on the balancing market with associated requirements [27].

What differentiates the products on the balancing market for primary control is mainly the frequency interval in which they are activated [28]. FCR-N is used during normal operation and is activated automatically at frequency deviations $|\Delta f| < 0.1$ Hz, i.e. when the system frequency lies within the interval $49.9 < f < 50.1$ Hz. The activation is linear, as explained in section 4.2 and bids are placed symmetrically, i.e. equal capacity for both up and down regulation. The actor providing FCR-N must guarantee a continuous supply of the reserve for the procured time period.

FCR-D is used when disturbances occur and is activated linearly, but is, unlike FCR-N, not symmetrical. Up and down regulation can be provided independently and bids are placed separately. FCR-D is activated automatically at frequency deviations $0.1 < |\Delta f| < 0.5$ Hz. FCR-D (up) is activated when the system frequency lies within the interval $49.5 < f < 49.9$ Hz and FCR-D (down) is activated when the system frequency lies within the interval $50.1 < f < 50.5$.

In case linear activation is not possible stepwise activation is permitted with the requirement of 50% activation within 5 seconds and 100% within 30 seconds (FCR-D) or 63% activation within 60 seconds and 100% within 3 minutes (FCR-N). All requirements are summarized in figure 4.3. Providers of FCR are compensated according to pay-as-bid pricing for cleared capacity. For activated energy, FCR-D is not compensated, while FCR-N is compensated according to up and down regulating prices [28]. Cleared capacity is the capacity for which the bid was accepted and activated energy is the energy which was actually used.

aFRR is activated when the frequency deviates from the nominal value of 50 Hz, and participating units receive control signals at time intervals of 10 seconds, as explained in section 4.2. To provide aFRR on the balancing market for secondary control, the actor offering the reserve must guarantee a reaction time of no more than 30 seconds, and be fully activated before 5 minutes, from that the TSO requests activation. The market for procuring aFRR is currently national and compensation for cleared capacity is based on marginal pricing, while activated energy is based on up and down regulating prices [29].

Activation of mFRR is currently done manually by the TSO and bids are accepted continuously as the reserves are needed. A provider of mFRR is required to fully activate the reserve within 15 minutes from that the TSO requests it, and is compensated for the provided balancing energy according to marginal pricing.

An example of how the different balancing reserves are activated due to a disturbance can be viewed in figure 4.4. Historically, hydro power production units have been the main providers of balancing power on the balancing market in Sweden, and still are [30].

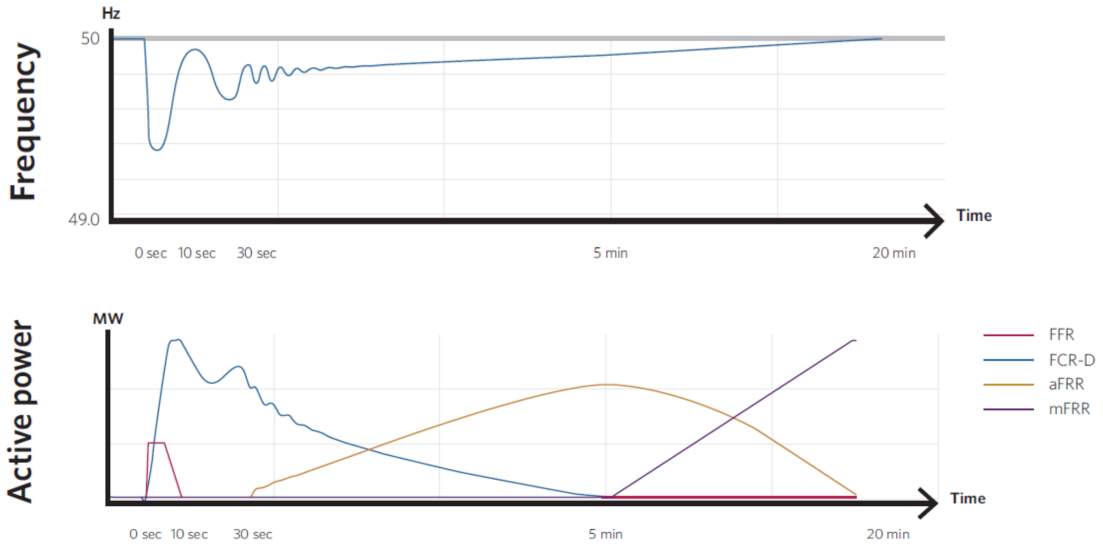

Figure 4.4: Example of how different balancing reserves are activated due to a disturbance [20].

Markets for frequency related ancillary services

When operating an electric power system, several technical aspects and requirements have to be satisfied. In addition to energy balance, previously described and traded on energy and balancing market, several other ancillary services are needed to ensure a robust and well functioning system. To improve economic efficiency, some of these services are procured by mainly TSOs on specific markets for ancillary services.

Fast frequency reserves (FFR) does not quite qualify to be included in the primary control, but is rather an ancillary service designed to compensate for the decreasing share of rotational mass in the system. It was implemented in the Nordics in May 2020 and each country has its own market [20]. The procurement of FFR in Sweden is done both on a seasonal basis and two times per week, and is based on forecasted need each hour. Participating units are compensated according to marginal pricing.

Another ancillary service is the assurance of sufficient production capacity. Different countries use different strategies to handle this, where two common ones are market-wide capacity mechanisms and strategic reserves market [31]. Sweden, together with several other European countries, uses strategic reserves procured by the TSO on a capacity market in order to assure sufficient production capacity and consumption reduction are made available for the TSOs during winter [26]. Some economists consider strategic capacity reserves a more economic alternative than the

market wide capacity mechanisms, but it is still under debate, and is strongly regulated in the EU regulation on the internal market for electricity (EU 2019/943) [31]. In practice, most of the Swedish strategic reserves consist of Karlshamnsverket, an oil-fueled condensing power plant with a nominal power of 660 MW, and some consumers which are prepared to shut down temporarily to reduce consumption, together adding up to 750 MW in Sweden and 611 MW in Finland [22].

A recent event in SE3 is close to an ideal example which illustrates how the different balancing reserves are activated in order to balance the system after a severe fault. Due to a three-phase short circuit fault during maintenance work north of Stockholm, and malfunctioning system protection resulting in a delay in fault clearance, the voltage level dropped in the whole region [32]. This caused both nuclear reactors Forsmark 1 and 2 to disconnect from the grid. Figure 4.5 shows measured frequency data from the time of the event [33]. Until the fault was cleared, the braking electrical load (torque) decreased and the frequency increased immediately, visible as a peak above 50 Hz at 06:40. When thereafter Forsmark 1 and 2 disconnected from the grid, the frequency dropped dramatically and FFR and FCR-D reserves were activated, stabilizing the frequency which reached a frequency nadir (minimum) of 49.3 Hz. aFRR and mFRR reserves were activated to restore the frequency to its nominal value. The measured frequency data is comparable to the example in figure 4.4, and the graph showing activation of reserves can be applied to this as well.

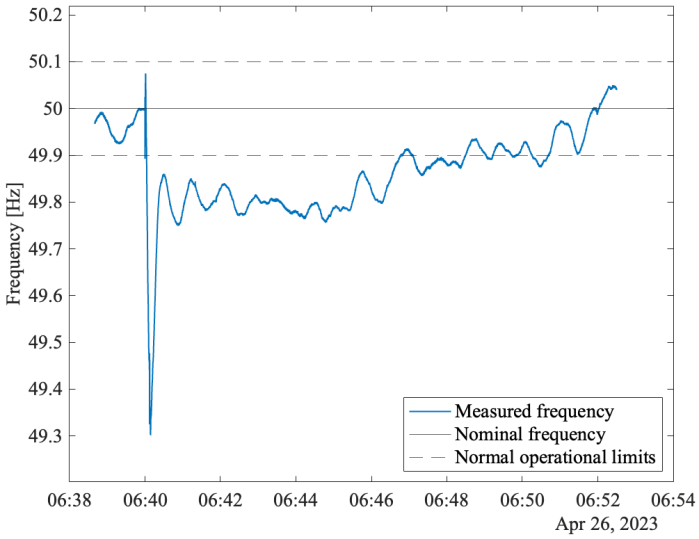

Figure 4.5: Measured frequency in the Nordic synchronous area showing disconnection of two nuclear power units at 06:40. This was preceded by a voltage dip induced by a short circuit, causing lower breaking electrical torque in (4.2), and thus increasing frequency immediately before the nuclear reactors were disconnected.

4.2.3 Responsibilities

A well functioning market ensures planned balance for each TP, but has no real time operational responsibility. Sustaining the instantaneous power balance is a task for the TSO. In Sweden, Svk is the one responsible for maintaining a reliable system operation, which entails sustaining the short-term power balance defined in section 4.1 [34]. This is done by trading on the balancing

market and procuring volumes of different reserves according to figure 4.3. It also entails quantifying the need to sustain this in both the near and distant future.

While Svk has the overall responsibility for the transmission system and maintaining a momentary power balance, there are several other actors involved in the work of balancing the system. Power producers and consumers present offers and bids of energy volumes through balance responsible parties (BRPs) to the market operator who determines the price, and the outcome of the Euphemia algorithm determines the scheduled power flows. The markets are operated by nominal electricity market operators, in Sweden consisting of Nord Pool and EPEX, with the majority of the trading taking place on Nord Pool [26]. To ensure the planned, hourly balance, the BRP has the duty to plan their operation and trade accordingly [35]. The energy volumes required to meet the predicted demand are procured on the day-ahead and intraday markets by energy REs, which are obliged to have a contract with a BRP if they do not themselves own the role [36]. For every power injection and power extraction point in the grid there must exist a BRP.

Today, the BRPs trade both on the day-ahead and intraday market as well as the balancing markets with FCR and FRR products. The services on the balancing market are procured by the one responsible for instantaneous balance, i.e. Svk in Sweden. Payments are settled based on bids and imbalances at injection and extraction points. Accountable for the Nordic imbalance settlement is eSett, owned by the four TSOs Energinet, Fingrid, Statnett and Svk [36].

Even though the Nordics are one synchronous area, they are still connected to the other synchronous areas in Europe, both physically and financially by the market. To coordinate the TSOs in Europe, ENTSO-E exists as an organization to produce guidelines and regulations for all power system actors. Their mission is to ensure ”the security of the interconnected power system in all time frames at pan-European level and the optimal functioning and development of the European interconnected electricity markets” [37].

4.3 Future trends

The overall and most evident trend is harmonization of markets, which is one action to facilitate the penetration of vRES in the power system. The European Commission Regulation (EU) 2017/2195 of 23 November 2017, also known as the Electricity Balancing (EB) regulation, establishes guidelines on electricity balance [38]. It contains detailed rules for the integration of balancing markets in Europe which will enable all interconnected countries to share their resources and thus improve the balance and increase the security o supply [38].

The foundation of a harmonized European balancing market is unified TPs and imbalance settlement periods (ISPs). This means Sweden, along with the other Nordic countries will undergo a transition from 60 minutes to 15 minutes on both energy and balancing markets [39]. This will allow trading of balancing services across all of Europe, which in turn will improve flexibility, price signals and management of the increasing imbalances. The ramping of dispatchable units around TP shifts causes power imbalances. These imbalances are predicted to decrease with the new settlement resolution [39].

In order to implement and enable the shorter ISP and fulfill the obligations in the EB regula-

tion, the Nordics developed the Nordic Balancing Model (NBM) [20]. The higher resolution in imbalance settlement will increase the workload and lead to less time to act for the operators, which is why the AOF, mentioned in section 4.2, was developed as a part of the NBM.

The EB regulation also results in the current role of BRP being divided into BRP and balance service provider (BSP) [8]. The BRP will have financial responsibility of possible imbalances that may arise, while BSPs are market participants providing FCR, aFRR and mFRR [40]. This differentiation will foster effective competition and enable more actors to enter the balancing market.

With a higher share of vRES power production the variability in generated electricity will increase, and will consequently bring variability and uncertainty to power system operation and planning [41]. Matching this variability with a flexible demand side alters the traditional way of thinking about the power system and its multiple actors. Returning to the grindstone example in section 4.1, where the previous philosophy has been to adjust the power injected to the system to satisfy the demand, the upcoming philosophy is to reconcile power production and consumption to each other, corresponding to the grinder and the cranker listening to each other in this metaphor.

Chapter 5

Quantitative study 1 - development of a network simulation tool

As proposed in section 4.2.2, it gets complicated to address the power balance over long periods of time. Consequently, a first approach to study balancing in a future power system of 2045 is to limit the TP resolution to 60 minutes, as in Svk's LMA scenarios.

On basis of this relatively low time resolution, the purpose of this quantitative study 1 (QS1) is to develop a tool, suitable for grid simulation analyses. As starting point, an existing network model of the Nordic synchronous area, further described in section 5.1, and the Svk LMA data are used. The model is updated in several ways to be capable of running load flow simulations using the LMA data, explained in section 5.2. This is automated with a Python script to run time series of load flows and process the resulting data series, described in section 5.3.

The outcome expectation of this quantitative study is a useful tool for further grid simulation studies with a geographical perspective, making a network model and input data accessible for future projects, while also gaining knowledge about grid simulations and scripting in Python. Examples of how the tool can be used will be shown in section 5.4, and this will be further discussed in section 5.5. In present state, the model is suitable for load flow simulations and static analysis, but requires further improvements to work for dynamical studies.

5.1 Nordic 44

Power systems are in general large and complex to model and analyze. The immense number of nodes and components in a detailed modeled network require a lot of computational power. Simplified network models that still are detailed enough to capture the properties of the complete network are needed. Nordic 44 (N44) is a test network of such character and models the Nordic synchronous area using 44 nodes [42].

Figure 5.1 shows the Nordic 44 network as a single line diagram distributed geographically next to a map of the actual transmission network in the Nordics. It is quite evident that the Nordic 44 model is heavily simplified. It does however capture the most important traits of the actual system. The large nuclear and hydro power production units in Sweden are well geographically

represented, as are the power lines connecting them. The voltage level is 420 kV throughout the network in Sweden and Finland, while Norway has both 420 kV and 300 kV voltage levels.

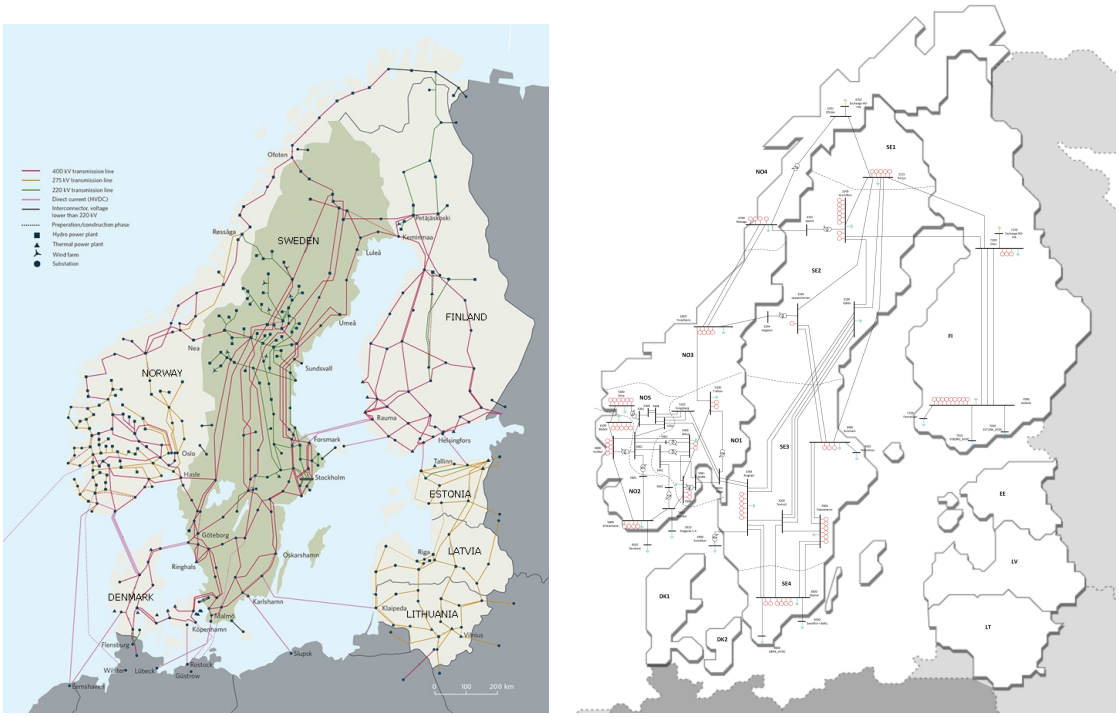

(a) Map of the actual Nordic transmission system network [43].

(b) Map of the Nordic transmission system network as represented in the Nordic 44 test model [44].

Figure 5.1: Maps of the Nordic transmission system network.

The Norwegian part of the grid is modeled in more detail due to the model being created in Norway at the Norwegian University of Science and Technology [42]. In the model, the Oskarshamn node serves as a swing bus, since the generator with the largest capacity is connected to this. HVDC links are modeled as loads connected to a separate node.

Notable is that the bidding zones in N44, as defined in the single line diagram in figure A.1 in appendix A, do not add up with the actual BZs for Norway and Finland. Finland is, for example, divided into two bidding zones, whilst in reality there is only one zone.

5.2 Nordic 46

Since one purpose of this thesis is to study future power system scenarios, the N44 test network is insufficient in its representation of the future Nordic synchronous system. Therefore, some updates are *necessary* to be able to dispatch the input data and obtain convergent load flow simulations, while some updates are made to *improve* the representation of the scenarios. The single line diagram of the updated model named Nordic 46 (N46), can be seen in figure A.2 in appendix A.

With the production categories described in section 3.3, the original Nordic 44 necessitates

more components to handle solar, onshore and offshore wind production, and vRES curtailment. Therefore, solar and wind power plants are added to all nodes with existing production or consumption, together with a load object representing vRES curtailment, which in practice reduces the vRES production in the software since it is connected to the same bus bar as the vRES production. This update is necessary in order to dispatch all production and obtain a convergent simulation, but also an improvement to get a better representation of the reality and a step towards running dynamic simulations, where vRES production can be modeled based on their dynamic characteristics. The updates in N46 are visible for comparison with N44 in figure 5.2.

In the LMA scenario data, all components are present in every BZ. The N44 model has not included units of both thermal and hydro power production in every BZ, meaning all components in the LMA data cannot be dispatched. Necessarily, a synchronous generator representing thermal power production is added to every BZ lacking this type of production unit, and likewise a synchronous generator representing hydro power production is added to every BZ lacking that type of production unit. If the BZ consists of more than one node, the new synchronous generator is placed at an arbitrary node in the BZ. Depending on the number of synchronous generators already connected to the node receiving a new generator, the principles for voltage control at the node is modified differently. If only one generator is connected, this alone is responsible for voltage control at the node. In order to make the new generator contribute to this control in a cooperative manner, a station controller necessarily needs to be added to the node. This enables all connected synchronous generators to collectively control the voltage level in a proportional way. If more than one synchronous generator is connected to the node receiving an additional generator, a station controller already exists, and the new generator thus only needs to be added to this, though it is still a necessary intervention.

In both N44 and N46, voltage is controlled through synchronous generators only, by dispatching reactive power. In N46, wind and solar PV power generating units have a predefined and constant power factor of one, i.e. they only inject active power to the grid. In the LMA scenario EF, the share of renewable power production from vRES is by far larger than today. Consequently, when these units do not contribute to voltage control, BZs with a significantly low share of power production originating from synchronous generators cannot sustain acceptable voltage levels in all associated nodes. In some nodes, the voltage risks dropping dramatically enough to cause a voltage collapse. In order to prevent this kind of event, by sustaining close to perfect voltage levels at all nodes in the model, two necessary measures are taken. Firstly, limits regarding reactive power dispatch are ignored for all synchronous generator in the model. Secondly, synchronous compensators are added to five selected nodes. These are synchronous generators participating in voltage control without injecting any active power to the grid. These measures are motivated and discussed in section 5.4.

The N44 model has several nodes with more than one load per node. In N46, these are reduced to one load per node to improve clarity and legibility of the model, without undermining the dynamic properties of the model. Of similar reason the numerous synchronous generators are kept, since they contribute with properties that are important in dynamical simulations.

The Nordic synchronous area have several internal and international HVDC connections, and some of them are connected to the same node in the Nordic 46 model. To improve clarity and

legibility, the structure with separate nodes for HVDC connections, represented as loads, is kept, yielding four new nodes. In order to avoid unnecessary components, the HVDC connecting nodes 8600 Baltic Cable and 8700 Svepol are merged to one node, and the same procedure is done for 7010 Fennoskan and 7020 Estlink HVDC. With removal of two nodes and addition of four to the initial 44 nodes results in a total of 46 nodes, and is the reason for the updated version being named Nordic 46. Examples of this can be seen by comparing figures 5.2a and 5.2b, and all the changes are visible in figures A.1 and A.2 in appendix A.

When performing load flow simulations, power lines are to some extent allowed to be loaded over their rated current. However, to obtain more realistic results, the rated capacity is adjusted on several BZBs according to what Svk predicts in their *System Development Plan* [8]. Here it should be mentioned that no updates in transfer capacity are made neither inside BZs nor outside Sweden, but this mainly affects the line loadings in % and barely not the power flows. This is partly due to the BZBs being physical bottlenecks in transfer capacity, and the internal capacities are thus less problematic, but also because of lack of information regarding BZ internal reinforcement.

Based on the BZ definitions in the N44 model, there exists an AC interconnection between the node 3249 Grundfors in SE1 and 7100 Oulu in FI1. In N46, 3249 Grundfors is by definition included in SE2, which is an improvement to better represent the actual BZs. Consequently, the connection between 3249 Grundfors and 7100 Oulu becomes invalid, since no AC connection between SE2 and FI exists in reality. This line is therefore disconnected in the N46 model, as can be seen in figure A.2 in appendix A.

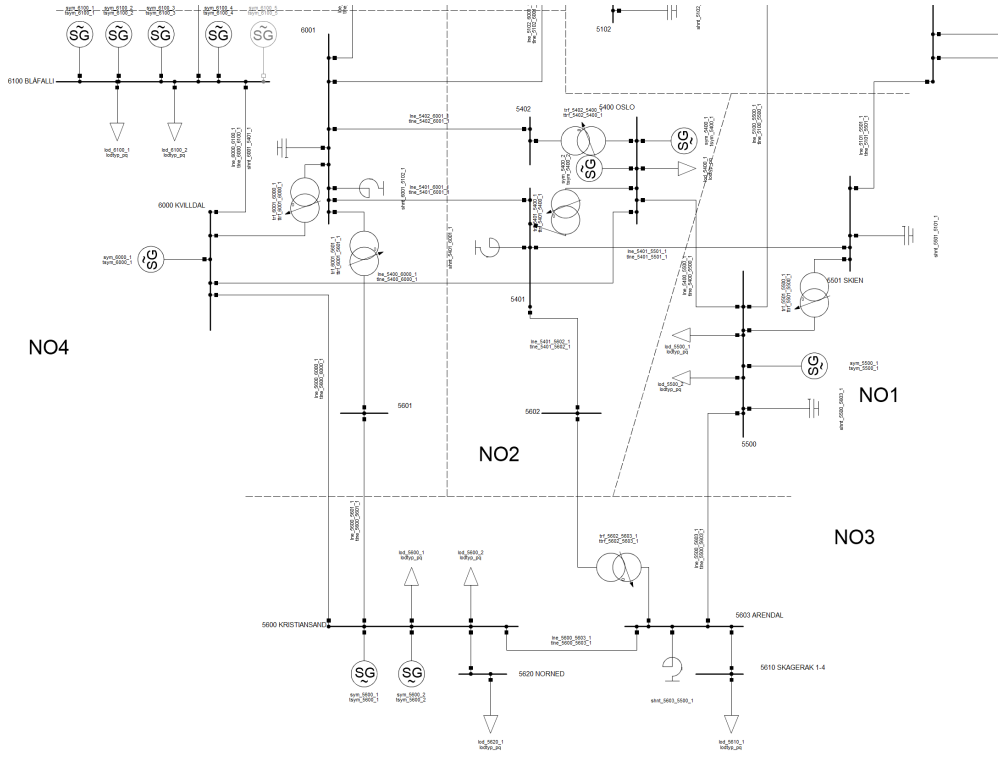

(a) Part of the N44 single line diagram showing the south part of Norway.

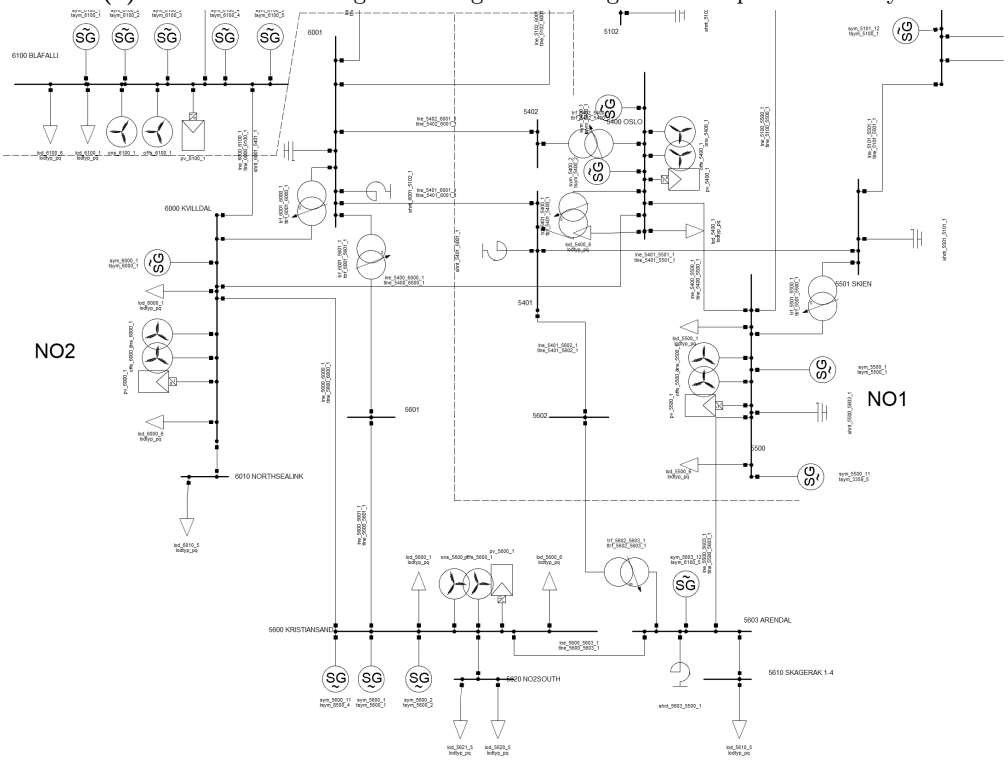

(b) Part of the N46 single line diagram showing the south part of Norway. Note the added vRES generating units at node 6000 Kvilldal, the added load representing a HVDC connection at node 5620 NO2SOUTH and the addition of a synchronous compensator at node 5603 Arendal.

Figure 5.2: Part of the N44 and N46 single line diagram which can be compared in order to notice changes and updates that have been made.

5.3 Implementation

The software used to simulate load flows on the Nordic 46 network model is PowerFactory (PF), developed by DIgSILENT. In order to perform an extensive number of load flows simulations consecutively based on the time series i the LMA scenario data, a Python script is developed to automate the process. An overview of how this process is implemented is depicted in figure 5.3.

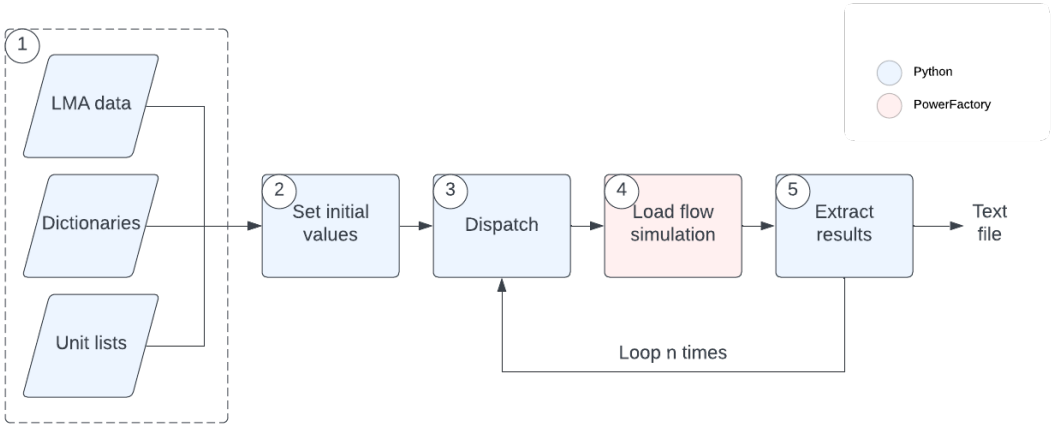

Figure 5.3: Flow diagram of the simulation process.

Reading from left to right, the initial three boxes contained within box 1 in figure 5.3 represent input data and structuring of objects. The LMA data is sorted into tables labeled by BZ. The PF objects subject to change during a load flow simulation need to be linked to their respective alias, which are stored in lists. These three parts build up the fundamental structure of how data is stored and accessed.

Each simulation process is initialized by defining power factors for all load objects, i.e. consumption loads, curtailment loads and HVDC loads. This is represented in box 2 in figure 5.3. The load flow simulations are looped as many times as there are data points in the time series. Before each load flow simulation is initiated, the LMA data is dispatched onto the network model utilizing the structure for access represented in box 1. The LMA data is divided by BZ, but has no further geographical granularity. The dispatch of data within a BZ is done according to equation (5.1), where *object* corresponds to the type of unit which the component data is linked to, e.g. hydro power production is linked to hydro power turbines. According to (5.1), the component data is evenly distributed on all objects in a BZ. Since there is a difference in the number of generators connected to each of the nodes, this difference thus results in more generation being allocated to a node with more generators. In for example SE3 this means that Ringhals will produce more electricity compared to Oskarshamn. The dispatch procedure is represented with box 3 in figure 5.3.

$$\text{Component}_{\text{object}} = \frac{\text{Component}_{\text{BZ}}}{\text{Nbr of objects in BZ}} \tag{5.1}$$

Once all data is dispatched, the load flow simulation is performed in PF. The process is represented in box 4 in figure 5.3. Finally, relevant result figures are stored before the next loop is initiated, which is represented with box 5 in figure 5.3.

5.4 Examples

To illustrate the performance of the model and load flow simulations, time series from LMA scenario EP are used. Figure 5.4 shows a histogram of the flows from SE1 to SE2, i.e. BZB 1, and the flow from SE3 to SE4, i.e. BZB 4. Both the flows as presented in the LMA data (yellow) and the resulting flows from the load flow simulations on N46 (blue) are presented. Both the simulations in PF and the LMA data include network losses, meaning the PF simulations, which are based on LMA data, count these losses twice. To compensate for this, the simulated losses in PF are subtracted from the result. In figure 5.4a, the discrepancy between the flows in the LMA data and the flows from the load flow simulations, is larger than in figure 5.4b. The reason for the discrepancy is strict capacity constraints on transmission between BZs existing in the LMA scenarios, i.a. yielding the spike at -3200 MW seen in figure 5.4a, and not in the N46 model. This difference in transmission constraints results in different power flows, and for BZs with multiple AC interconnections this difference is more prominent. This explains the discrepancy in figure 5.4a being larger than in 5.4b, since SE1 is connected to three other BZ through AC transmission, while SE4 (which in the N46 model includes DK2) only has one AC interconnection to another BZ.

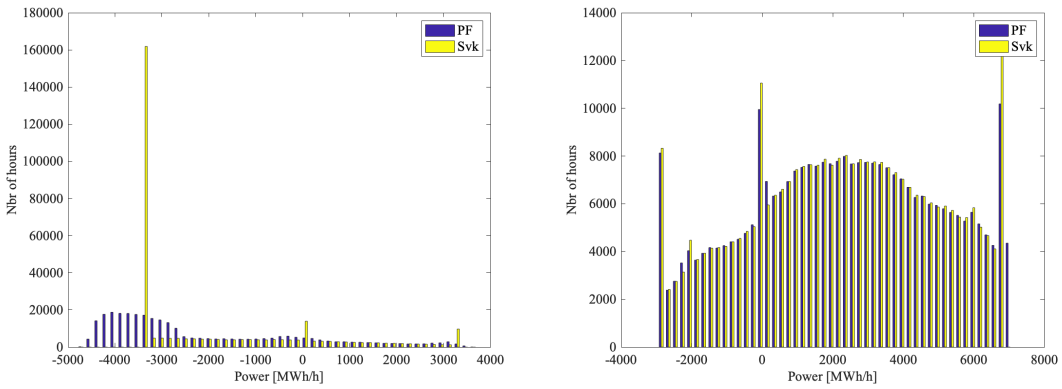

(a) Active power flow from SE1 to SE2 (BZB 1). **(b)** Active power flow from SE3 to SE4 (BZB 4).

Figure 5.4: Histograms showing active power flows over a BZB based on data from all 35 weather years from scenario EP. Blue bars are the result from simulated flows and yellow bars are based on Svk LMA scenario data.

The voltage in every node is sustained due to synchronous generators not being restricted in how much reactive power they can dispatch. This is however not enough, which can be seen in the upper bar plot in figure 5.5, where several nodes have a minimum voltage below the desired lower limit of 0.95 p.u. Adding synchronous compensators at selected nodes improves the voltage stability, as can be seen in the lower bar plot in figure 5.5. One exception is the two synchronous compensators, one at Hjälta and one at Tenhult, present already during the simulation resulting in upper bar plot. This is due to voltage collapses occurring without them being placed there, yielding non convergent load flow simulations.

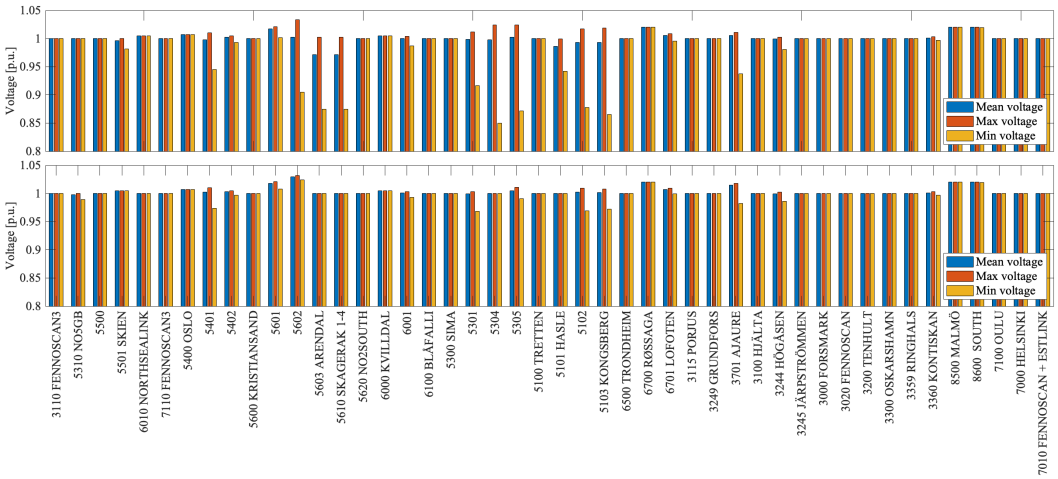

Figure 5.5: Voltage characteristics in the 46 nodes for TP simulations weather years 1986 and 1987, indicating a significant improvement when synchronous compensators with voltage regulation have been added (below). One can note that the voltage controllers in nodes 8500 Malmö, 8600 South and 6700 Røssaga are set to 1.02 p.u., explaining the sligly larger bars.

Since there is no limit to how much reactive power all synchronous generators in the model can generate, it can be of interest to study the total amount of reactive and active power injected into the grid. Figure 5.6 shows active power, reactive power and power angle, defined as cosine of the angle between these two quantities. The ratio is reasonable and gives an indication of how much reactive power is needed in order to sustain nominal voltages in the system.

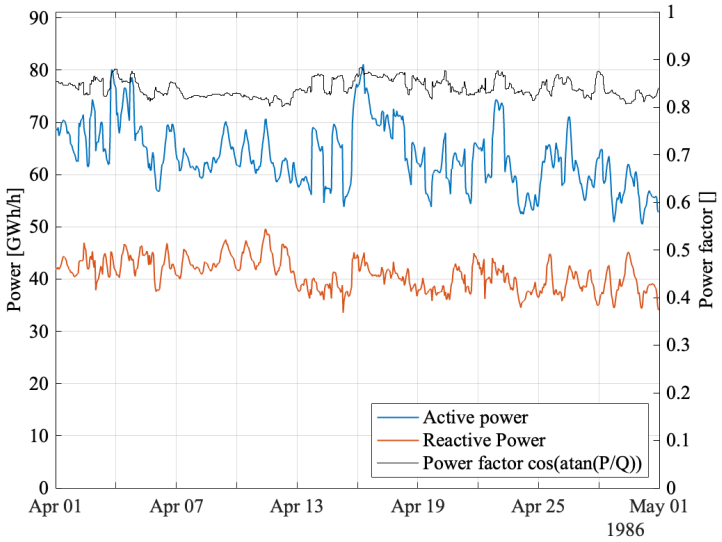

Figure 5.6: Active and reactive power injected to the system from generating units.

5.5 Analysis and discussion

The resulting tool is a foundation which can both be used in its current state and be further developed. Remarks on what to be aware of, followed by suggested improvements are presented here.

Although this tool has been developed based on the LMA scenario data from Svk, it is not limited to perform load flows solely from time series data with hourly resolution. It is indeed possible to input data of finer granularity, but the user must be aware of the limitations with performing load flow simulations, which are static. Dynamic behaviour will have a greater impact on the system and be more prominent with a higher resolution. Conclusions must thus be drawn with care when increasing the time resolution in the input data.

The dispatch of load and generation is somewhat naive in the current implementation. For BZs containing only one node, this is not a problem, but with multiple nodes in a BZ the distribution of inhabitants, industry and types of power generation is neglected. This leads to inaccuracy of power flows within a BZ. As an example, SE2 has offshore wind power production which is currently divided equally between the three nodes 3249 Grundfors, 3245 Järpströmmen and 3100 Hjälta, while it is obvious no offshore wind exists in the area around 3249 Grundfors and 3245 Järpströmmen.

As explained in section 5.2, synchronous generators alone control the voltages in all nodes and are not limited in reactive power dispatch. Since the focus of this thesis is on balancing and not stability, this implementation is deemed sufficient for performing load flow simulations. It is obviously an incorrect representation of reality, but is possible to improve and develop further.

5.6 Further development

One first and direct suggestion for improvement is to handle the geographical power dispatch in a less naive way. Mapping installed capacity of every power production type to the area represented by a node, will yield a distribution more like reality. In terms of consumption, it gets more complicated. The data on consumption is unfortunately not very transparent, i.e. it is not possible to differ between industry consumption, household consumption and flexible use of electricity. This makes the dispatch of power demand in an accurate way close to impossible, if the data is not pre-processed in a similar fashion as was done with the RES data in section 3.3. Given consumption data sorted by type of end user, the dispatch can be made based on the same principle as for power generation of different types.

For the N46 model, a useful development would be to make it adaptable for dynamic simulation. This would enable more extensive studies and consequently make the model a more accurate representation of reality. Making the N46 model adaptable for dynamic simulations would entail a more detailed specification on wind and solar PV power production units, including reactive power dispatch and control characteristics.

Chapter 6

Quantitative study 2 - investigation of the need for balancing power on a minute scale

One purpose of this thesis is to quantify the need for balancing power in a future scenario of the power system in 2045, with high degree of electrification, and investigate how an electrified vehicle fleet can contribute to the balancing. As was concluded in chapter 4, the fundamental definition of power balance is momentarily producing and consuming equal amount of power. In reality, this entails forecasts followed by energy volumes traded on energy markets, which is complemented with balancing markets to compensate for variability within the TPs. This variability is omitted in scenario data such as the one produced by Svk, since the resolution is limited to a TP. To more accurately address the question of future needs of balancing power, the fundamental definition of power balance must not to be forgotten.

Real, historic data of power flow on a HVDC interconnection between DK2 and Germany, and wind power generation in Denmark, can be seen in figure 6.1 [33]. The hourly mean is also presented in the figures, and when comparing this to the high resolution measurements, it becomes evident that TP resolution is insufficient.

In this second quantitative study (QS2) the need for balancing power in higher temporal resolution is investigated in future scenarios of year 2045. The initial structure is to high extent based on the article *Estimating the Future Need for balancing power Based on Long-Term Power System Market Simulations*, written by Henrik Nordström [45], where the time series presented in section 3.2 are interpolated based on their characteristics. These high resolution time series are added up in each bidding area to form what previously was a balance, but the added characteristics contribute to high resolution imbalances. If there are available transmission capacities, opposite imbalances in neighboring BZ can to some extent cancel each other. During this "netting", a positive imbalance in one BZ compensates for a negative imbalance in an adjacent BZ if possible, yielding a minimized total imbalance. It is the methods for interpolation and optimization proposed in the article that are used in this chapter.

Since one of the research questions is to investigate the potential of V2G contributing to future

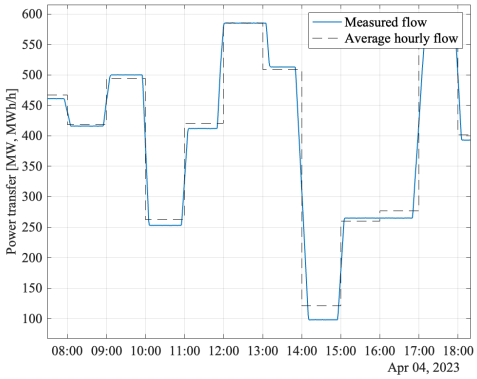

(a) Example of measured flow through the HVDC connection from BZ DK2 to Germany, where the ramping around TP shifts is clearly visible.

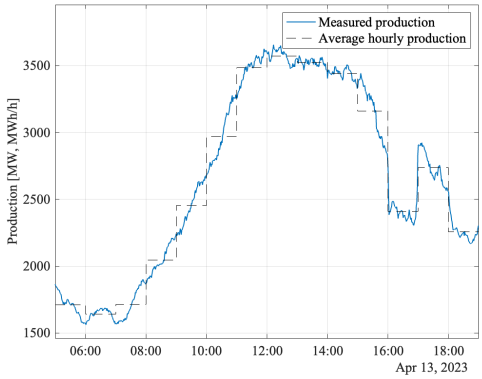

(b) Example of measured wind power generation in Denmark with minute resolution and averaged hour resolution.

Figure 6.1: Examples of measured data of a HVDC flow and wind power production.

power system balancing, a model of aggregated electric vehicles is added in section 6.4 to provide balancing services with V2G. With significant uncertainties in transportation sector, two scenarios are used to investigate the potential of balancing through V2G.

The case study is based on data from April weather year 2015. This month contains the largest TP shift in the total data set, i.e. the largest change in power production, including net export, from one TP to another in Sweden. Since TP shifts to high extent contribute to the imbalances, this was chosen as motivational basis for the chosen month.

6.1 V2G

The amount of EVs and plug-in hybrid EVs (PHEVs) in Sweden grows exponentially [46]. The share of newly registered vehicles being EVs or PHEVs (from here denoted only EVs) went from 4% in 2016 to 45% in 2021 [47]. The battery and associated power electronics in an EV are resources that can be utilized for more than just the charging and propulsion of the vehicle. It is this idea of multipurpose that has defined the concept of vehicle to everything (V2X), which include e.g. V2G, vehicle to home (V2H) and vehicle to building (V2B). V2G is, based on bidirectional charging, a technology which can support the grid by acting as a large, distributed battery, both to be charged and discharged in a way that benefits the grid. From the grid perspective, the advantage with V2G is that the charging of the vehicle can be controlled fast enough to qualify for all services on the balancing market described in chapter 4 [30].

The potential is, in theory, huge. Assuming 3 million EVs discharging with 10 kW, this results in an aggregated power output of $3 \cdot 10^6 \cdot 10$ kW $= 30$ GW, which can be compared to the peak load hour in Sweden of 25-30 GW [48]. However, in practice, several challenges exist which have to be addressed in order for EVs to be of any service to the grid.

To make the V2G solution possible, the exchange of information between the EV and the charging infrastructure will have to increase. Both software and hardware will need standardization, which is currently under development in the ISO 15118 standard [49]. Also the local distribution

networks will have to become more digital in order to send relevant control signals to the charging EVs [49]. Somewhere between the EV battery and the grid an inverter is needed. A crucial decision for V2G to become a commercial solution is whether the inverter should be placed in the car or the charging box [49].

EVs are distributed all over Sweden and when parked for charging they connect to the local distribution grids. To abate the national need of flexibility, aggregators coordinating larger sets of EVs are important to make V2G possible [30]. Along with this, local control signals, the ancillary services and market models need to develop and adapt to the new balancing solutions and technologies such as V2G [49]. In the end, to what extent the owners of the flexibility resources, i.e. EV batteries, are willing to participate will highly depend on the degree of economical feasibility for the service [50].

6.2 Higher time resolution - quantifying the need for balancing power

The definitions and notations used here are based on those presented in [45]. Imbalances are divided into TP *energy* imbalances and *power* imbalances. The TP energy imbalance is defined as the difference between the energy during one TP in the original data from Svk, and the energy during one TP in the simulated high resolution data. Assuming perfect forecast in the data from Svk, the TP energy imbalance is zero. Continued work has been carried out by Henrik Nordström where these forecast errors are considered [41], but for the purpose of this thesis it is sufficient to assume no forecast errors. The power imbalance is defined as the instantaneous (=minute) difference between the assumed constant power in the data from Svk and the simulated high resolution data. In contrast to the TP energy imbalance, the power imbalance is not necessarily zero.

As introduced in the beginning of this chapter, the first step is to interpolate the time series based on their characteristics. The two main categories are controllable components, i.e.

- hydro power production g^{hy},
- nuclear power production g^{nu},
- other thermal power production g^{th},
- load curtailment g^{lc}, and
- HVDC connections z^{dc},

and continuously varying components, such as

- consumption d,
- offshore power production g^{off},
- onshore power production g^{on},
- solar PV power production g^{PV}, and
- vRES curtailment g^{RES}.

The controllable components are set to a constant level during most of the trading period, and when there is a shift the production or export is ramped with a predefined ramping rate before and after the TP shift occurs. The varying components are not controllable and vary in a relatively smooth pattern on BZ level. Therefore these are modeled with a cubic spline interpolation. The deterministic AC flows, $\hat{z}^{ac}_{\hat{t},a}$, are assumed to be constant during each TP.

As in formula (3.2) in section 3.1, the high resolution time series, denoted with hats, are added together in (6.1), defining the deterministic need for balancing power $\hat{w}^{bal}_{\hat{t},n}$. The residual in formula (3.2), here denoted $\hat{r}_{\hat{t},n}$, is non-zero. Since it is not expected to occur, there is no obvious way of interpolating it, and it is therefore assumed to be hourly constant also in high resolution. Here A represents the set of BZ interconnections, n denotes the set of bidding zones, and flow is defined from BZ $n1$ to BZ $n2$.

$$\begin{aligned}\hat{w}^{bal}_{\hat{t},n} = &-\hat{g}^{hy}_{\hat{t},n} - \hat{g}^{nu}_{\hat{t},n} - \hat{g}^{th}_{\hat{t},n} - \hat{g}^{lc}_{\hat{t},n} - \hat{g}^{off}_{\hat{t},n} - \hat{g}^{on}_{\hat{t},n} - \hat{g}^{PV}_{\hat{t},n} + \hat{g}^{RES}_{\hat{t},n} + \hat{d}_{\hat{t},n} - \hat{r}_{\hat{t},n} + \\ &+ \sum_{a\in\{A:n1=n\}} \hat{z}^{ac}_{\hat{t},a} - \sum_{a\in\{A:n2=n\}} \hat{z}^{ac}_{\hat{t},a} + \sum_{a\in\{A:n1=n\}} \hat{z}^{dc}_{\hat{t},a} - \sum_{a\in\{A:n2=n\}} \hat{z}^{dc}_{\hat{t},a}\end{aligned} \tag{6.1}$$

6.2.1 Interpolation

In this subsection all the TP energy time series are interpolated to high resolution time series based on their characteristics. The general notation is that variables without hat are defined in TP time resolution of 60 minutes, while variables with hat, $\hat{*}$, are defined in high time resolution of 1 minute. Accordingly, T is the last entry of the time series in question in TP resolution, e.g. the hour 23:00-23:59 of a day, while $\hat{T}$ refers to the last high resolution entry of the time series, i.e. minute 23:59:00-23:59:59 in the example. Subsequently, $\hat{T}/T = 60$ is the time resolution factor.

Ramping controllable components

The controllable components are set to a constant basic power during each trading period, with exception of short ramping periods around TP shifts. These ramping periods, $C_{t\to t+1}$, in high resolution time units before and after each TP shift are calculated as in (6.2), with ramping rate r as a percentage of maximum power w^{max}. The power is linearly interpolated from w_t to $w_t + 1$ during these ramping periods.

$$C_{t\to t+1} = \min\left(\frac{|w_{t+1} - w_t|}{r \cdot w^{max}} \cdot \frac{1}{2}, \frac{\hat{T}}{T} \cdot \frac{1}{2}\right) \tag{6.2}$$

For HVDC interconnections, restrictions exists regarding ramping. From one hour to the next, the increase or decrease in flow is limited to 600 MW [51]. This restriction is assumed to already be accounted for in the input data. Furthermore, the ramping rate, r, i.e. the speed at which the flow is changed, is limited to 30 MW/minute [51]. This restriction thus becomes relevant in the case of minute resolution data, and is implemented in the interpolation.

For the remaining ramping components, the ramp rates are set according to table 6.1 and are based on values presented in [45]. Regarding hydro power, all the facilities are here assumed to be controllable, i.e. no run-of-the-river hydro power plants are simulated.

Table 6.1: Ramp rates of controllable components.

Hydro, Load curtail [$\%g_{max}$/min]	Thermal [$\%g_{max}$/min]	Nuclear [$\%g_{max}$/min]
5	3	1.5

Varying components through cubic spline interpolation

The varying components depend on constantly varying factors such as weather conditions or consumption decisions made by individuals. In a relatively low geographical resolutions, e.g., bidding areas as in this case, these components aggregate to relatively smooth, constantly varying time series, and this property is well captured by a cubic spline interpolation [52]. This is done by using the Matlab cubic `spline` function with t-resolution time series and an offset to $t + 0.5$, to better match the hourly balance. Here one should note that the `spline` function does not ensure equal TP energy after interpolation.

Ensuring TP energy balance

When using the above described interpolation methods TP energy errors are likely to occur, so that the high resolution intra-TP energy $\frac{T}{\hat{T}} \sum_{\hat{t}=\frac{\hat{T}}{T}(t-1)+1}^{\frac{\hat{T}}{T}t} \hat{w}_{\hat{t}}$ differs from the low resolution energy w_t. To maintain the intra-TP energy balance, [45] and [53] propose the following iterative algorithm.

First, the intra-TP energy difference h is calculated as in (6.3) for iteration i.

$$h_t^i = w_t - \frac{T}{\hat{T}} \sum_{\hat{t}=\frac{\hat{T}}{T}(t-1)+1}^{\frac{\hat{T}}{T}t} \hat{w}_{\hat{t}}^i \tag{6.3}$$

Then the sum square error is defined as $e^i = \frac{1}{2}\sum_{t=1}^{T}(h_t^i)^2$, and if e^i is greater than a maximum tolerance level e_{tol}, an updated TP-resolution time series $a_t^{i+1} = a_t^i + h_t^i$ is formed and used as input to the interpolation function in question $f(*)$, as in (6.4). The scheme essentials are summarized in Algorithm 1.

$$\hat{w}^{i+1} = f(a^{i+1}) \tag{6.4}$$

Algorithm 1

Input: Low resolution time series w
Output: High resolution time series $\hat{w}$
Initialization: $a^1 = w$
while $e^i > e_{tol}$ **do:**
$a^{i+1} = a^i + h^i$
$\hat{w}^{i+1} = f(a^{i+1})$
$h^{i+1} = w_t - \frac{T}{\hat{T}} \sum_{\hat{t}=\frac{\hat{T}}{T}(t-1)+1}^{\frac{\hat{T}}{T}t} \hat{w}_{\hat{t}}^i$
$e^{i+1} = \frac{1}{2}\sum_{t=1}^{T}(h_t^i)^2$
$i = i + 1$

Examples of the ramping and cubic spline interpolations are shown in figure 6.2a and 6.2b respectively, with and without Algorithm 1.

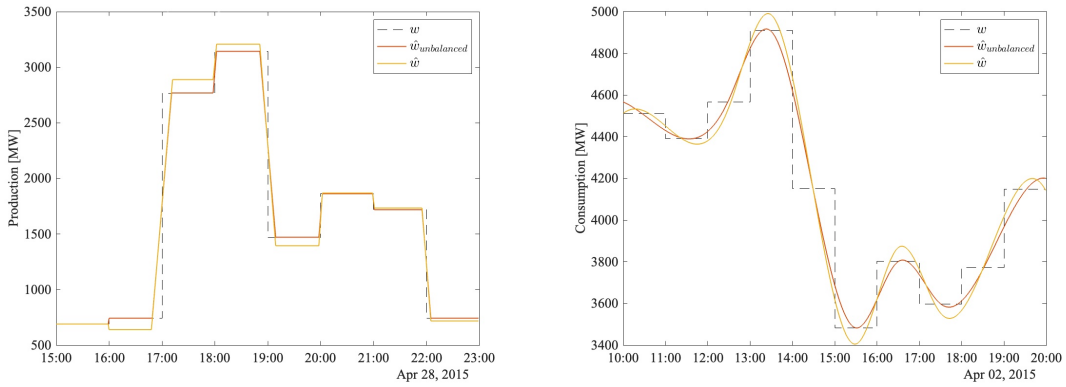

(a) Example of interpolation for controllable component: ramped hydro power in SE2.

(b) Example of interpolation for varying component: continuously varying consumption in SE1.

Figure 6.2: Examples of interpolation methods with the low resolution data as dashed line as reference. $\hat{w}_{unbalanced}$ represents the interpolated time series, and for $\hat{w}$ Algorithm 1 has been used to eliminate the intra-TP energy error.

An illustrative comparison can be made between figures 6.1 and 6.2, indicating adequate interpolation results. The notable difference is a high frequency component, visible in the measured wind generation data but not in the interpolated time series, that otherwise follows the same structure.

6.2.2 Netting and optimization

The need for balancing power is so far given by (6.1). At any time $\hat{t}$, the need for balancing power can be positive in one BZ and negative in an adjacent BZ. Given that available transmission capacity (ATC) between the two BZs exists, there is a possibility of minimizing the total need for balancing power by netting these flows. As proposed in [45], an optimization problem can be formulated which minimizes the total need for balancing power in the system. In addition to minimizing the total need for balancing power, it is also relevant to minimize the total amount of netting AC flows, $\hat{z}^{ac,net}_{\hat{t},a}$, to some extent. The objective function to be minimized is described by (6.5), where α is the cost of the flows and *postnet* indicates the need for balancing power after netting flows.

$$\sum_{\hat{t}=1}^{\hat{T}} \sum_{n \in N} |\hat{w}^{bal,postnet}_{\hat{t},n}| + \alpha \sum_{\hat{t}=1}^{\hat{T}} \sum_{a \in A} |\hat{z}^{ac,net}_{\hat{t},a}| \tag{6.5}$$

The netting AC flows are limited by ATC in both directions, yielding the constraints formulated in equation (6.6). $\underline{\text{ATC}}$ is the lower limit and $\overline{\text{ATC}}$ is the upper limit, which are based on the net transfer capacity (NTC) and deterministic AC flow for each BZB.

$$\underline{\text{ATC}}_{\hat{t},a} \leq \hat{z}^{ac,net}_{\hat{t},a} \leq \overline{\text{ATC}}_{\hat{t},a} \qquad \hat{t} = 1, ..., \hat{T}, \quad a \in A \tag{6.6}$$

To ensure power balance, the constraint formulated in (6.7) is added, containing the need for balancing power before netting flows, $\hat{w}^{bal}_{\hat{t},n}$, from (6.1).

$$\hat{w}^{bal}_{\hat{t},n} + \sum_{a\in\{A:n1=n\}} \hat{z}^{ac,net}_{\hat{t},a} - \sum_{a\in\{A:n2=n\}} \hat{z}^{ac,net}_{\hat{t},a} - \hat{w}^{bal,postnet}_{\hat{t},n} = 0 \tag{6.7}$$

The objective function (6.5) should be minimized subjected to the constraints in (6.6) and (6.7), where $\hat{w}^{bal,postnet}$ and $\hat{z}^{ac,net}_{\hat{t},a}$ are the variables to be optimized. The optimization problem is rewritten to be solved linearly and is performed in Python, using Gurobi [54]. The output from the optimization is the total need for balancing power after optimal netting of flows, $\hat{w}^{bal,postnet}$.

6.3 V2G implementation

The model of the aggregated electric vehicles is based on aggregated battery size, charging/discharging power and time connected to a charging station, as well as predefined state of charge (SoC) requirements. Vehicles participating in the V2G solution are assumed to have some battery capacity at disposal only for V2G. This implies that when they return from driving, they return with the same amount of energy available for V2G as they left with. Compared to updating available battery capacity simply from number of parked vehicles, giving the model memory yields a more realistic behavior.

For each time instant, $\hat{t}$, an algorithm checks if, and to what extent, the aggregated EV model can reduce the need for balancing power. A decision tree for how the algorithm works is depicted in figure 6.3.

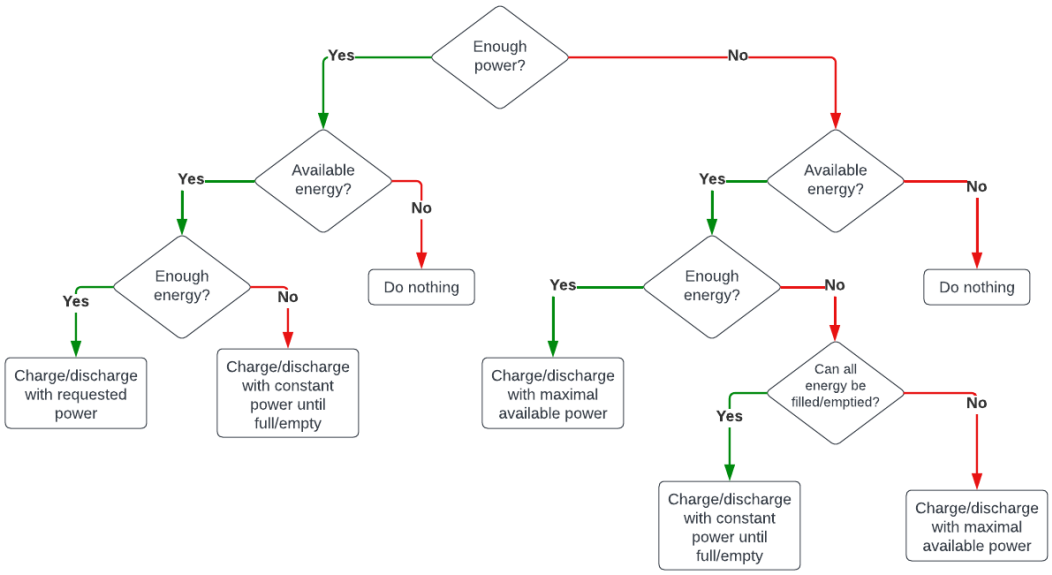

Figure 6.3: Decision tree describing how an aggregated EV battery model participating in a V2G solution is controlled. The decisions are made with respect to the aggregated battery capacity and power in each BZ at every time step.

To illustrate how the battery operates, an example of the remaining need for balancing power after the V2G implementation is presented in figure 6.4, together with the need for balancing power after netting of AC flows, minimum and maximum charging/discharging power and SoC for both parked and driving vehicles. Box A in figure 6.4 illustrates how the whole imbalance

remains, due to the battery being fully charged when the need for balancing power is negative. It can be seen by looking at box B in figure 6.4, that when the absolute need for balancing power, at any time $\hat{t}$, is larger than the maximum charging/discharging rate, and the battery SoC has not yet reached its limit, the need for balancing power is reduced to maximum charging/discharging rate of the aggregated battery. If, at any time $\hat{t}$, both enough charging/discharging power and battery capacity is available, the need for balancing power is reduced to zero, which can be seen an example of in box C in figure 6.4.

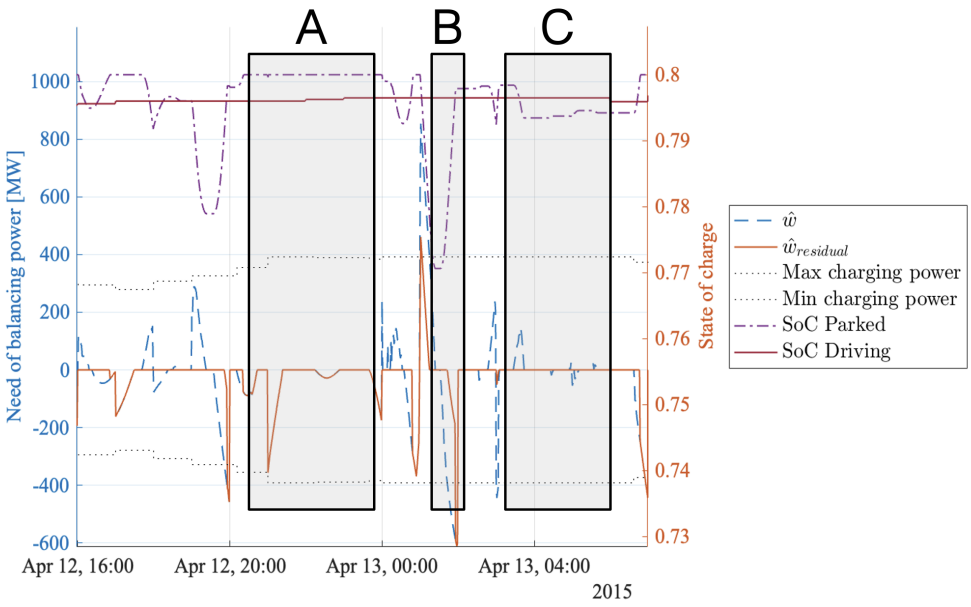

Figure 6.4: Example of need for balancing power $\hat{w}$ and residual after V2G $\hat{w}_{residual}$, plotted together with charging power limits and state of charge. Negative need for balancing power imply an excess of energy in the BZ.

6.4 Case study: 2 automotive scenarios

A topic currently debated is if or when autonomously driving cars will be introduced on large scale [55]. This will strongly affect the potential for V2G used as frequency control or grid balancing. Therefore, two scenarios of interest are simulated in a case study. Here, all vehicles are assumed to have battery electric drive train, and no electric road or fuel cell vehicles are considered. Further, only cars are treated, but same functionality could be implemented similarly for heavy vehicles.

Scenario 1: ***Privately owned vehicle fleet*** **(PO).** In this scenario the passenger vehicles are driven by persons as today. Further, they are assumed to mainly be owned by the users, i.e. households or companies. This entails a high number of cars with a geographical distribution similar as today [56, 57]. Some vehicles are assumed to not be electric, especially in northern Sweden [47]. In this scenario the use of a car is relatively low, so that the V2G availability will be high, indicated in figure 6.5[58]. The average battery capacity is expected to be relatively small [59], and since many vehicles will be parked at home or at work, their charge and discharge power will be relatively low. The participation degree β is assumed to be high, since there might be incentives in terms of balancing markets to participate in for aggregated V2G. The minimum

SoC accepted is set relatively low, since most vehicles are not assumed to use their whole battery capacity regularly. The upper SoC limit is set to 0.8, since the speed of charging decreases when the SoC approaches 1 [60]. All numerical values are presented in table 6.2.

Scenario 2: ***Autonomous mobility*** **(AM).** In this scenario autonomously driving cars are assumed to be implemented to high extent. This means that the passenger cars will be used somewhat like taxis, i.e. owned by commercial companies or car pools and used on demand [61]. With high probability, this implies an efficient use of vehicles for transportation, and consequently relatively low availability for V2G services, shown in figure 6.5. On the other hand, a high share of the cars are probably battery electric vehicles with a large average battery capacity [62] and high charging powers [63]. Regarding the degree of participation and acceptable minimum SoC, no reasonable values have been found in literature, so they are set as in table 6.2. Neither a fleet size or geographical distribution of the vehicles were found. Therefore the crude assumption was made that the demand of transportation work remains the same as in the PO scenario. With a maximum vehicle usage of 85 % of the total fleet during peak demand, the total number of vehicles is calculated as in equations (6.8) to (6.10), and then set with the same geographical distribution.

$$\text{Vehicles driving} = (1 - \text{Share of vehicle fleet available for V2G}_{PO}) \cdot \text{Nbr of vehicles}_{PO} \tag{6.8}$$

$$\text{Nbr of vehicles}_{AM} = \frac{\text{Vehicles driving}_{max}}{0.85} \tag{6.9}$$

$$\text{Share of vehicle fleet available for V2G}_{AM} = \frac{\text{Nbr of vehicles}_{AM} - \text{Vehicles driving}}{\text{Nbr of vehicles}_{AM}} \tag{6.10}$$

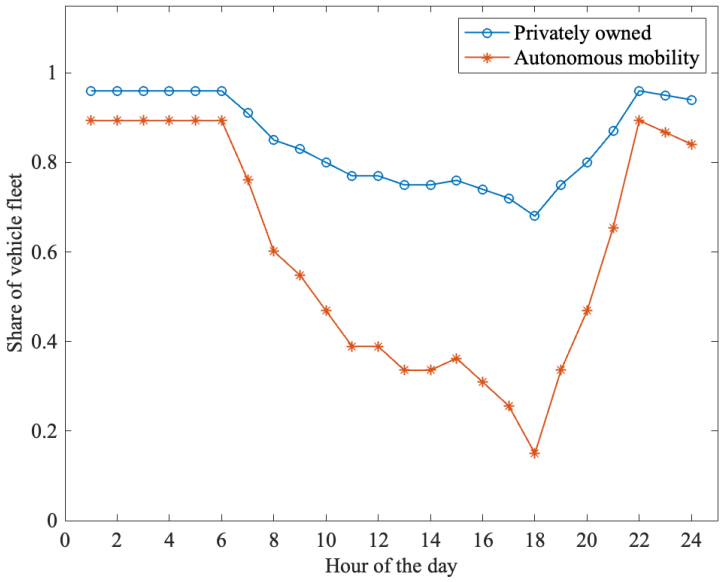

Figure 6.5: Availabilities for the Autonomous mobility and Privately owned cases throughout the day. From [58] and equation (6.10)

Table 6.2: Input parameters for V2G simulations.

Input parameter	**PO**	**AM**
Nbr of vehicles (Tot)	6 500 000	2 450 000
- SE1	259 713	97 892
- SE2	521 725	196 650
- SE3	4 253 564	1 603 267
- SE4	1 464 998	552 191
Share of EVs per BZ	-	-
- SE1	0.5	0.7
- SE2	0.7	0.85
- SE3	0.9	0.95
- SE4	0.85	0.9
Battery size [kWh]	40	100
Charging power [kW]	7	20
Availability	See figure 6.5	
Participation β	0.9	0.7
Max SoC	0.8	0.8
Min SoC	0.5	0.6
Initial SoC	0.65	0.7

6.5 Case study results

The decrease in need for balancing power due to netting and flows between adjacent BZs is illustrated in figure 6.6a. Further, figure 6.6b shows the decrease of need for balancing power with the two V2G scenarios applied. Both the netting and the two V2G solutions present an obvious reduction of imbalances.

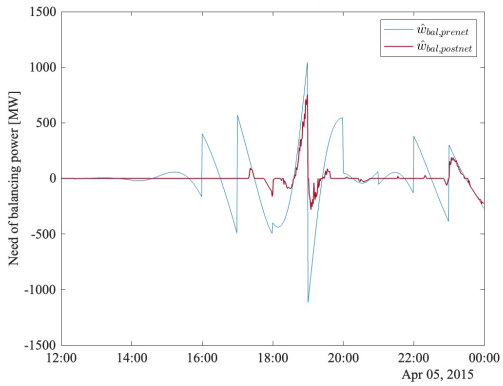

(a) Need for balancing power before and after netting flows.

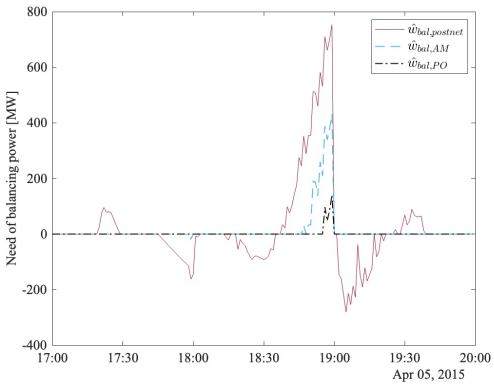

(b) Need for balancing power after netted flows as well as with the two V2G scenarios.

Figure 6.6: Need for balancing power during 12 hours in April 2015 in SE1 for scenario EF.

Figure 6.7 shows the SoC of vehicles parked and driving for each BZ, based on scenario PO. In all BZs but SE3, the battery saturates to either its maximum och minimum level.

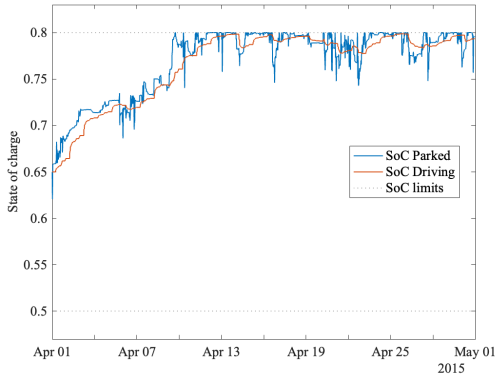

(a) SE1

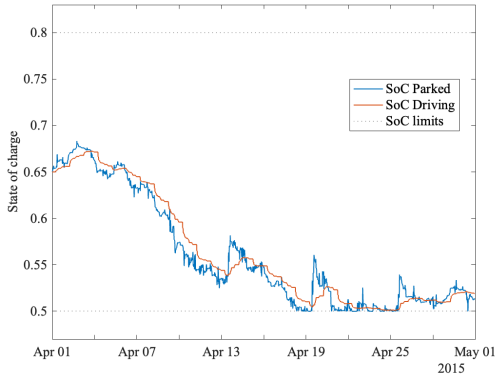

(b) SE2

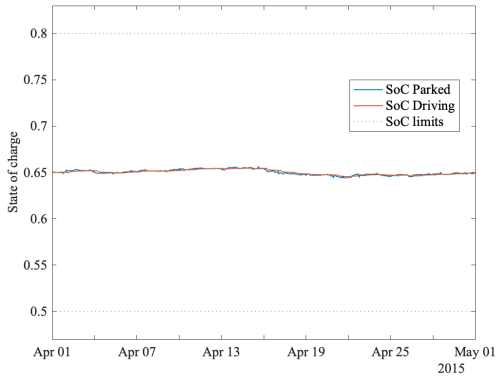

(c) SE3

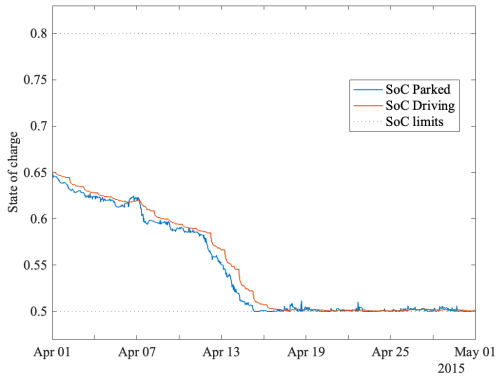

(d) SE4

Figure 6.7: SoC during April 2015 scenario EF, PO

Presented in table 6.3 are some key figures for comparison of the need for balancing power before netting flows, after netting flows and with the two V2G scenarios applied, using data from scenario EF.

Table 6.3: Imbalance key figures for April weather year 2015 scenario EF for stages prenet (PrN), postnet (PoN), Autonomous Mobility (AM) and Privately Owned (PO), per bidding area.

BA	min $\hat{w}^{bal}$ [MW]				max $\hat{w}^{bal}$ [MW]				mean($\lvert\hat{w}^{bal}\rvert$) [MW]				$\hat{w}^{bal} = 0$ [% of time]			
	PrN	**PoN**	**PO**	**AM**	**PrN**	**PoN**	**PO**	**AM**	**PrN**	**PoN**	**PO**	**AM**	**PrN**	**PoN**	**PO**	**AM**
SE1	-1 600	-999	-999	-912	1 458	1 154	549	858	103	29	6	7	0	62.29	93.54	92.92
SE2	-3 052	-2 154	-198	-746	2 663	1 788	1788	1788	178	46	3	4	0	63.45	98.01	97.15
SE3	-1 958	-1 426	0	0	1 568	1 220	0	0	196	70	0	0	0	58.25	100	100
SE4	-2 193	-2 193	0	-410	1 902	1 902	1499	1499	169	74	10	14	0	44.58	92.99	91.36

Similarly as in table 6.3, table 6.4 shows the same key figures but for scenario EP.

Table 6.4: Imbalance key figures for April weather year 2015 scenario EP for stages unnetted (PrN), netted (PoN), Autonomous mobility (AM) and Privately owned (PO), per bidding area.

BA	min $\hat{w}^{bal}$ [MW]				max $\hat{w}^{bal}$ [MW]				mean($\lvert\hat{w}^{bal}\rvert$) [MW]				$\hat{w}^{bal} = 0$ [% of time]			
	PrN	**PoN**	**PO**	**AM**	**PrN**	**PoN**	**PO**	**AM**	**PrN**	**PoN**	**PO**	**AM**	**PrN**	**PoN**	**PO**	**AM**
SE1	-2 461	-1 977	-1 977	-1 977	2 738	2 218	1 661	2 074	70	19	5	6	0	58.93	88.40	88.76
SE2	-2 413	-1 286	0	-376	2 207	1 444	1 133	1 444	83	26	2	2	0	62.91	97.93	97.07
SE3	-1 339	-962	0	0	1 622	948	0	0	129	61	0	0	0	48.42	100	100
SE4	-1 728	-1 116	0	-27	1 468	1 231	0	0	86	50	0	0	0	43.19	100	100

6.6 Discussion

Regarding the assumptions, method and results presented in this chapter, there are several matters relevant for a more profound discussion. The three central areas of interest for further discussion are interpolation, netting of opposite power imbalances and the vehicle to grid application.

6.6.1 Interpolation

Regarding the interpolation, the used `spline` function gives a smooth and realistic shape. One could criticize the rapid power changes or what seems to be overshoots, e.g. as in figure 6.2b, but these precipitous sections originate from the quickly alternating consumption input depicted in dashed stairs in mentioned figure, and the overshoots are consequences of Algorithm 1, in order to maintain TP energy balance. These relatively large and rapid changes are in themselves a consequence of the current trading periods of 60 minutes. With 15 minute TPs, as described in section 4.3, the varying components will probably remain unchanged due to weather conditions and behavioral patterns, but the controllable components can be traded with higher time resolution, reducing the rampings and thus the total need for balancing power seen in figure 6.6a.

In section 6.2 the unexpected TP energy residual is set to be hourly constant. There is no obvious reason to this, and the mainly periodic pattern indicates a controllable component, such as a battery storage. The residual could thus be interpolated through e.g. ramping or splining, but

this is a relatively small component, and would barely affect the overall results and conclusions.

6.6.2 Netting and optimization

The result of netting flows is clearly visible in figure 6.6a, where the need for balancing power has decreased significantly. The figure only shows SE1 during a few hours in April, but studying the columns presenting $\hat{w}^{bal} = 0$ for PrN and PoN in table 6.3, the same result is valid for the whole month and all BZs as well. It can also be verified by studying the column presenting the absolute mean value for PrN and PoN. By looking at the extreme values and comparing PrN and PoN, conclusions can be drawn regarding limited transfer capacity and coinciding need for balancing power in adjacent BZs. The minimum need for balancing power is the same in SE4 before and after netting flows, suggesting either no available transfer capacity from SE3 and DK2 or all three BZs having an excess of power during the given minute. Overall, large peaks remain in all BZs after netting, which concludes that some source of balancing power is needed.

Studying figure 6.6 once more, the need for balancing power obtains a high frequency variation after netting flows. One could question if these high frequency components are problematic in the sense of control characteristics, but a possible solution (already suggested in [45]) is to minimize the deviation in flow from one time instant to the next, $|z_{t+1} - z_t|$, instead of just the absolute flow, $|z_t|$.

Before netting, the need for balancing power is zero over time within a BZ, due to the hourly energy balance ensured by Algorithm 1. However, when netting flows, some BZs will over time export more energy, while others import more energy. This causes the need for balancing power to tip in either a positive or negative direction, thus saturating the battery state of charge. In all but SE3, the aggregated battery capacity is insufficient to meet the balancing power demand, visible in figure 6.7, even for such a short period of time as a month. Since the aggregated battery in SE1 saturates to its upper limit, the need for balancing power is consequently predominantly negative. Netting thus resulted in SE1 having an excess of energy. The same reasoning is legitimate for the other BZs as well. Two possible questions arise from this conclusion, suggesting two alternative approaches to the problem. The first being if the balancing power should be provided within each BZ and not through transmission between them, and the second being improving the control of the battery. With the current implementation, SE3 is the only BZ where V2G would work over time, due to the large number of EVs and net zero imbalance over time.

6.6.3 V2G implementation

When designing the battery control scheme, the first decision is whether to use predictive or real time feedback control, i.e. regulate on a forecast or an existing error such as frequency deviation or power imbalance. In this straightforward control scheme the current need for balancing power is used as control signal, and something similar could be obtained by using frequency deviation in a physical implementation. A predictive scheme could use a more intelligent approach and prioritize minimizing imbalance peaks, but would require a prediction of need for balancing power. Other control signals could be incorporated in the battery control, such as energy and balancing

market prices or actual power limits.

As mentioned, an issue with the current battery control is that the battery SoC saturates relatively quickly as shown in figure 6.7. With a more sophisticated battery steering, such as predictive, this could be prevented. A similar feature could also probably be obtained by adding an integrating part on the battery control, e.g. by striving to keep the battery state of charge away from the SoC limits, which would "save" some battery capacity for peak demands.

As figures 6.4 and 6.6b indicate, the battery control implementation tries to eliminate as much of the power imbalance as possible until the aggregated batteries saturate. This entails relatively long periods with no need for balancing power while there is still available capacity, but when the battery gets saturated, the need of balancing reaches a spike immediately. This gives an undesired residual that is difficult to compensate for with other balance resources. If instead a peak shaving controller, with e.g. predictive or integrating features, would be used, the residual need for balancing power obtained after V2G could be smoother, and thus easier to handle for other frequency control or even on the energy market with 15 minute TPs.

The overall methodology used to decrease the need for balancing power is in theory a two-step implementation. Netting flows, followed by simulating V2G. In reality, it is reasonable to assume these are two actions performed simultaneously. This is yet another suggestion for an improvement in the battery control, i.e. take into account both possible transmission between BZs and the local assets.

6.6.4 Case study

The min $\hat{w}^{bal}$ and max $\hat{w}^{bal}$ values in tables 6.3 and 6.4 clearly show an improvement after netting, which can also be seen in the $\mu(|\hat{w}^{bal}|)$ and $\hat{w}^{bal} = 0$ key values. For this primitive battery control, the min $\hat{w}^{bal}$ and max $\hat{w}^{bal}$ are not appropriate as comparative figures, since the V2G cannot take care of the peak values when the battery SoC is saturated, but the $\mu(|\hat{w}^{bal}|)$ and $\hat{w}^{bal} = 0$ indicates a significant improvement. With one of the proposed improvements on the battery control scheme, the magnitudes of the max and min values would decrease even more.

As can be seen in tables 6.3 and 6.4, the comparative figures from the two automotive scenarios are relatively similar. The higher charging power limit, battery size and share of EVs in the AM scenario is compensated by the higher number of vehicles, lower SoC limit and degree of participation in the PO scenario, but both scenarios result in a significant improvement. Actually, the lower total charging power in the AM scenario makes the batteries "last longer" before saturation, whose aggregated size is significantly smaller than in the PO scenario. However, the overall result is that the PO scenario performs just as well or better than AM in all cases except min $\hat{w}^{bal}$ in SE1 EF scenario and $\hat{w}^{bal} = 0$ in SE1 in EP scenario.

The AM scenario involves a disruptive shift in technology. In this chapter, it has been assumed that the transportation demand pattern in 2045 is similar to today's, but this is not necessary or even likely since behavioral patterns, price and availability might change if cheap transportation is offered through driverless vehicles with high user availability. In this scenario it is also possible

that the autonomous vehicles will swap their used batteries to fully charged ones, thus changing the fundamental principles of V2G.

In this chapter only battery electric vehicles are considered, and they are assumed to make up the whole passenger car fleet. In reality, other technologies for electrification, such as electric roads or hydrogen fuel cells, are feasible, which would reduce the aggregated battery capacity remarkably, but also change the availability. This simulation is also limited to include only passenger cars, but the V2G functionality could also be implemented on electric buses and trucks.

Chapter 7

Conclusion

This chapter serves as closure of the report through summary, analysis and discussion of previously presented material, rather than drawing further conclusions. Several interesting extensions of this work and associated topics of interest have arisen during this project, of which some are presented in section 7.2.

Returning to the research questions presented in 1.2, the interpolation based on technology characteristics resulted in significant power imbalances on minute scale, which cannot be seen in the time series with hour resolution. The quantified need for balancing power is presented in section 6.5. Furthermore, the V2G simulation indicates a great technical potential for abating these power imbalances.

7.1 Analysis and discussion

When studying the future scenarios of 2045, it is evident that the typical patterns in power production, consumption and balancing known today will change. The most obvious difference may lie in the way power is consumed, which currently follows a very repetitive pattern depicted in figure 2.2. The blue curves in figure 3.2 look much less repetitive and two reasons for this are the new industries and the flexibility they bring. Today, electricity is used almost regardless of what it costs, which is an approach future electricity intensive industries cannot have in order to work financially. What is seen in the LMA data is instead industries, alongside other users, consuming electricity when it is available, i.e. when the price is low. This is also visible in figure 3.2, where consumption peaks coincide with the stochastic vRES production peaks. Flexibility also enables consumers to enter the balancing market and further follow the variable power production, rather than expecting generation to follow consumption.

It is easy to notice the abnormal behaviour of the hydro power production in both scenario EF and EP. Today, hydro power is known to handle the residual load in the system due to its ability to store and generate energy whenever necessary, as well as act as the dominant provider of regulating power. As can be seen in figures 3.2c and 3.2d, Swedish hydro power production is in the 2045 scenarios characterized by long periods of constant dispatch, which is far from what would be expected in a power system with a large share of varying renewable power production. The most reasonable explanation for this lies in the market based simulation method used by Svk, which favor the low cost generation due to marginal pricing. This suggests the potential in hydro

power used to balance TP energies on the day-ahead and intraday markets, might instead be a greater asset as regulating power on the balancing market. On the other hand, there are other suggestions contradicting this. Following the trends discussed in section 4.3, more participants will enter the balancing market, and the ones offering their balancing services to the lowest price will be used. Even if hydro power were to provide regulating power at the lowest price, there are possible technical limitations. With higher variability, the rate at which a unit providing regulating power have to change its dispatch, will increase. If these changes in power dispatch are both rapid and frequent, this will cause mechanical tear in the hydro power plants. Since the vast majority of hydro power is located in SE1 and SE2, utilizing it as regulating power relies on available transfer capacity to cover the need for balancing power in SE3 and SE4. Further, with the new NBM mentioned in section 4.3, imbalances will be handled more locally through the CAs, and thus require local assets. Southern Sweden can consequently not solely rely on hydro power on the balancing market, which underlines the importance of the studies performed in chapter 6.

7.1.1 Time perspectives

A question of more general character is if the frequency control should be handled in real time with frequency measurements as today, or if the power imbalances can be predicted accurately enough to be used in a predictive control structure that avoids frequency deviations. Some imbalances, especially those arising from the controllable components that are ramped, are easy to predict, and could be handled with anticipation, which would reduce the deviations. A relevant observation on this topic is that the aggregated charging rate for V2G in a BZ, presented in section 5.3, is of comparable size to the volume requirements for reserves shown in figure 4.3, which relates the simulation results to practical numbers used in operation by Svk. The input parameters are intended to be as accurate as possible, but even if the premises and thereby following results would be somewhat optimistic, they clearly indicate that there is a technical potential for power system balancing with V2G.

On these topics, the emerging question is how a grid balancing V2G system is to be controlled. As mentioned, there would be some clear advantages with a central controller through e.g. the TSO, which is what has been used in QS2. Studying the imbalances on BZ level becomes relevant when the new NBM will be implemented based on CAs corresponding to these. On the other hand, with plentiful electric vehicles, geographically widely distributed, other challenges in terms of communication and security risks arise. On the contrary, local V2G controllers enables island operation, and the power imbalances are taken care of as local as possible. If V2G is to be commercialized, the incentives must involve economical aspects, and beyond frequency and forecasted power imbalance, both energy and balance market price could be input parameters for controlling the system.

Another topic related to this is on which market V2G is suitable. With fluctuating energy prices, vehicle owners or aggregators could benefit economically from buying electricity when the price is low and sell it back when the price is higher, and thus only participating on the energy only market. However, as shown above, V2G is maybe even more suitable for frequency control and ancillary services, but this requires commercialization through aggregators. On the balancing

market, V2G has the potential to meet the requirement for all products [30]. A question that calls for further studies is if V2G is a solution only to be traded on the balancing market as it is known today, or if this technology enables either alternative methods or markets, or both, for frequency control and power system balancing.

7.1.2 Other aspects

BESS solutions such as V2G cannot only be seen as an asset in the context of power balance and frequency control. Power electronic based units are characterized by rapid response times and high controllability, which can be used to compensate for the decreasing share of rotational energy through FFR, mentioned in chapter 4. Moreover, they can participate in voltage control through reactive power dispatch. The broad spectra of qualities obtained through high controllability creates incentives to enable for these technologies to be a part of the power system.

The entire QS2 is based on that the vehicle to grid concept is completely decoupled from the normal charging. This is indeed a coarse simplification, and it is done since the consumption data provided in Svk's simulations already contains flexible EV charging but no V2G. In reality, charging from grid and discharging to grid will not be completely decoupled, but the complete bidirectional charging will be handled by the same system. With consumption data divided into consumption categories, a different control structure could be built, that probably would be more complex but also more realistic.

With a larger share of the electricity production being weather dependent, the need for improved forecasts grows. The accuracy in forecasts naturally improves with shorter prediction horizons, which suggests an increase in volumes traded on the intraday market. There are however limits to these improvements, and errors will still persist. The simulations in chapter 6 do not take these forecast errors into account, and are consequently prone to under- or overestimate the total volumes of balancing energy. Regardless of this, the intra-TP variability remains and plainly states the need for balancing power omitted due to the limits in market TP resolution. Returning to the question of what role hydro power is to play in the future scenarios of the 2045 power system, the answer could lie in the compensation of hourly forecast errors, leaving rapid changes in dispatch to power electronic based units.

7.2 Future work

The backbone of this thesis is the perspective from which the power system has been studied, i.e. the future. As mentioned earlier, the future is hard to predict and scenarios are a useful tool for studies of this kind. The scope of this work has limited the number of scenarios to investigate, but it would be of high interest to apply other scenarios to the studies performed in both chapter 5 and 6, and compare the results.

All the suggested improvements of the tool developed in chapter 5 have already been mentioned there, but can be summarized to consist of a general ability to perform dynamic simulations and better resemble reality. Since it is defined as a tool, future work on the matter of chapter 5 would entail further studies utilizing this tool.

As pointed out in chapter 4, this thesis is being conducted in the middle of a transformation of the electricity markets as well as the concepts for power system balancing in general. In future studies, it would be interesting to see the effect of these changes on the results from QS2, e.g. how 15 minute TP resolution would affect the need for balancing power. Some improvements are suggested for the method in QS2 itself, both in the interpolation and in the implementation of the V2G battery model. A part of the interpolation consists of ensuring TP energy balance, which is based on the assumption of perfect forecasts. The method could be improved by accounting for these, which has already been done in [41]. The aim of the battery model is currently to eliminate the need for balancing power, but could be implemented to target corresponding large deviations in frequency instead, if using a predictive control approach as discussed in section 7.1.1. Developing a more intelligent battery control scheme is a future work of high interest, which probably would come with a translation of need for balancing power to frequency deviations. Another concrete suggestion for improvement of the V2G battery model is to implement two different types of charging connections, corresponding to fast charging and normal, low power charging.

Not only is the future of the power system uncertain, but the technology and human behavior is as well. The two scenarios presented in chapter 6 give two possible outcomes, but just as for the scenarios of the future power system, more could be studied regarding future transport constellations.

As discussed in section 5.5, the role of hydro power production in Sweden in the future scenarios of 2045 is somewhat unclear. Even though studies have been made regarding technical limits of hydro power units ramping, the question remains how hydro power and V2G could cooperate to reduce the need for balancing power.

Chapter 8

Bibliography

[1] J. D. Glover, T. J. Overbye, and M. S. Sarma, *Power System Analysis and Design 6th Edition*. Cengage Learning, 2017.

[2] Energimyndigheten, "Minskad elanvändning under 2022." `https://www.energimyndigheten.se/nyhetsarkiv/2023/minskad-elanvandning-under-2022-i-sverige/`, 2023 02. [Online, last accessed 2023-04-17] (In Swedish).

[3] Energimyndigheten, "Energy in sweden 2022, an overview," Tech. Rep. ET 2022:04, 2023.

[4] Energimyndigheten, "Energiläget 2022," Tech. Rep. ET 2022:09, January 2023. (In Swedish).

[5] Mimer, Svenska kraftnät, "Förbrukningsstatistik sverige." `https://mimer.svk.se/ProductionConsumption/ConsumptionIndex`, 2023 January. Online, last accessed 2023-04-17.

[6] Svenska kraftnät, "Om transmissionsnätet." `https://www.svk.se/om-kraftsystemet/om-transmissionsnatet/`, January 2023. [Online, last accessed 2023-05-10] (In Swedish).

[7] Svenska kraftnät, *Målet: Alltid maximal tillgänglig kapacitet i ledningarna.* `https://www.svk.se/press-och-nyheter/temasidor/tema-om-overforingskapacitet-och-tillganglighet/` [Online, last accessed 2023-02-06], 2021. (In Swedish).

[8] Svenska kraftnät, "Systemutvecklingsplan 2022–2031," 2021. (In Swedish).

[9] Svenska kraftnät, "Kortsiktig marknadsanalys 2021," Tech. Rep. 2022/3235, December 2022. (In Swedish).

[10] Svenska kraftnät, "Långsiktig marknadsanalys 2021," Tech. Rep. 2019/3305, May 2021. (In Swedish).

[11] A. Wilkinson and R. Kupers, "Living in the futures," *Harvard business review*, vol. 91, no. 5, pp. 118–127, 2013.

[12] Svenskt Näringsliv, "Kraftsamling elförsörjning - Scenarioanalys 290 TWh," June 2022. (In Swedish).

[13] Svenska kraftnät, *Unpublished LMA simulation data.* Personal communication, 2021.

[14] Henrik Nordström, *Python script*. Personal communication, 2023.

[15] ENTSO-E, "Data from ENTSO-E PECD (Pan European Climate Database)." https://zenodo.org/record/3702418#.Y-tFLXbMI2x, March 2020. [Online, last accessed 2023-02-10].

[16] "Nordic Grid Development Perspective 2021," November 2021.

[17] Fingrid, "Fingrid open data platform, frequency real time data." https://data.fingrid.fi/open-data-forms/search/en/index.html?selected_datasets=177, May 2023. [Online, last accessed 2023-05-23].

[18] ENTSO-E, "Nordic balancing philosophy," November 2021.

[19] ENTSO-E, "Load-frequency control and performance (appendix 1)."

[20] ENTSO-E, "Overview of frequency control in the nordic power system," March 2022.

[21] Nordic Balancing Model, "The nordic afrr capacity market went live 7th of december 2022!." https://nordicbalancingmodel.net/the-nordic-afrr-capacity-market-went-live-7th-of-december-2022/, December 2022. [Online, last accessed 2032-04-24].

[22] A. Khodadadi, L. Herre, P. Shinde, R. Eriksson, L. Söder, and M. Amelin, "Nordic balancing markets: Overview of market rules," in *2020 17th International Conference on the European Energy Market (EEM)*, pp. 1–6, IEEE, 2020.

[23] Svenska Kraftnät, "Electricity trade." https://www.svk.se/en/national-grid/operations-and-electricity-markets/electricity-trade/, March 2021. [Online, last accessed 2023-05-03].

[24] Svenskt Näringsliv, "PPA och elmarknaden, en rapport till svenskt näringsliv," September 2020. (In Swedish).

[25] Nord Pool, "EUPHEMIA Public Description - Single Price Coupling Algorithm." https://www.nordpoolgroup.com/globalassets/download-center/single-day-ahead-coupling/euphemia-public-description.pdf, October 2020. [Online, last accessed 2023-05-23].

[26] Energimarknadsinspektionen, "Sveriges el- och naturgasmarknad 2021," Tech. Rep. R2022:06, 2022. (In Swedish).

[27] Svenska kraftnät, "Information on different ancillary services." https://www.svk.se/en/stakeholders-portal/electricity-market/provision-of-ancillary-services/information-on-different-ancillary-services/, February 2023. [Online, last accessed 2023-05-08].

[28] Svenska kraftnät, "Villkor för FCR - Bilaga till Avtal om Balansansvar för el (Avtal 4620-4)," March 2023. (In Swedish).

[29] Svenska kraftnät, "Villkor för aFRR - Bilaga till Avtal om Balansansvar för el (Avtal 4620-4)," March 2023. (In Swedish).

[30] Power Circle, "Flexibilitet för ett mer stabilt och driftsäkert elsystem - en kartläggning av flexibilitetsresurser?," Decemeber 2022. (In Swedish).

[31] P. Holmberg and T. Tangerås, "Hellre effektreserv än kapacitetsmarknad," Tech. Rep. IFN Working Paper No. 1387, 2021, 2021 April. (In Swedish).

[32] Svenska kraftnät, "Driftströrningen den 26 april 2023," Tech. Rep. Svk 2023/1561, May 2023. (In Swedish).

[33] Morten Hemmingsson, *Unpublished frequency measurement data.* Personal communication, 2023.

[34] Svenska kraftnät, "Om systemansvaret." `https://www.svk.se/om-kraftsystemet/om-systemansvaret/`, December 2021. [Online, last accessed 2023-04-20] (In Swedish).

[35] Svenska kraftnät, "Balansansvarig." `https://www.svk.se/aktorsportalen/balansansvarig/`, March 2023. [Online, last accessed 2023-04-21] (In Swedish).

[36] eSett, "Nordic imbalance settlement handbook," April 2023.

[37] ENTSO-E, "Entso-e mission statement." `https://www.entsoe.eu/about/inside-entsoe/objectives/`. [Online, last accessed 2023-04-26].

[38] ENTSO-E, "Entso-e balancing report 2020," 2020.

[39] Svenska Kraftnät, "15 minuters tidsupplösning." `https://www.svk.se/utveckling-av-kraftsystemet/systemansvar--elmarknad/ny-nordisk-balanseringsmodell-nbm/15-minuters-tidsupplosning/`, April 2022. [Online, last accessed 2023-04-25] (In Swedish).

[40] Svenska kraftnät, "Utveckling av elmarknaden." `https://www.svk.se/utveckling-av-kraftsystemet/systemansvar--elmarknad/utveckling-av-elmarknaden/`, February 2023. [Online, last accessed 2023-04-28] (In Swedish).

[41] H. Nordström, L. Söder, and R. Eriksson, "Minute resolution multi-areawind power simulation to estimate future reserve needs," in *Accepted to PowerTech 2023*, (Belgrade, Serbia), 2023.

[42] Sintef, "The nordic 44 test network." `https://www.sintef.no/en/publications/publication/1701481/`. [Online, last accessed 2023-02-02].

[43] Svenska kraftnät, "Map of the national grid." `https://www.svk.se/en/national-grid/map-of-the-national-grid/`, March 2021. [Online, last accessed 2023-05-10].

[44] S. W. Nordhagen, "Reliability analysis of the nordic44 model and modelling of corrective actions in opal," January 2017.

[45] H. Nordström, L. Söder, and R. Eriksson, "Estimating the future need of balancing power based on long-term power system market simulations," in *Proceedings of 11th Bulk Power Systems Dynamics and Control Symposium (IREP 2022)*, (Banff, Canada), July 25-30, 2022.

[46] Power Circle, "Elbilsstatistik." `https://www.elbilsstatistik.se/elbilsstatistik`. [Online, last accessed 2023-05-12] (In Swedish).

[47] J. Barr and M. Topel, "Långsiktiga scenarier för introduktion av elfordon," Tech. Rep. 2022:899, Energiforsk, 2022. (In Swedish).

[48] Svenska kraftnät, "Kraftbalansen på den svenska elmarknaden, rapport 2022," Tech. Rep. 2022/879, May 2022. (In Swedish).

[49] Power Circle, "Vad är V2G - Vehicle to Grid?," February 2020. (In Swedish).

[50] DNV GL Energy, "Samhällsekonomiska kostnader och nyttor av smarta elnät," Tech. Rep. 208978, March 2021. (In Swedish).

[51] ENTSO-E, "Explanatory document for the amended nordic synchronous area proposal for ramping restrictions for active power output in accordance with article 137(3) and (4) of the commission regulation (eu) 2017/1485 of 2 august 2017 establishing a guideline on electricity transmission system operation," January 2021.

[52] Mathworks, "Cubic spline function." `https://se.mathworks.com/help/matlab/ref/spline.html`. [Online, last accessed 2023-04-13].

[53] M. Nilsson, L. Söder, and Z. Yuan, "Estimation of power system frequency response based on measured simulated frequencies," in *2016 IEEE Power and Energy Society General Meeting (PESGM)*, pp. 1–5, 2016.

[54] Gurobi Optimization, *Documentation*. `https://www.gurobi.com/documentation/` [Online, last accessed 2023-05-19], 2021.

[55] C. Ljungberg, "Hajpen som kom av sig: "helt självkörande bilar minst 10 år bort"." `https://www.di.se/nyheter/hajpen-som-kom-av-sig-helt-sjalvkorande-bilar-minst-10-ar-bort/`. [Online, last accessed 2023-04-12] (In Swedish).

[56] Energimyndigheten, "Scenarier över sveriges energisystem 2020," Tech. Rep. ER 2021:6, March 2021. (In Swedish).

[57] Trafikanalys, "Personbilar. antal i trafik efter ar och län." `https://www.trafa.se/vagtrafik/fordon/?cw=1&q=t10026|ar:2022|itrfslut|reglan~standardtable`. [Online, last accessed 2023-04-12] (In Swedish).

[58] M. Taljegard, L. Göransson, M. Odenberger, and F. Johnsson, "Impacts of electric vehicles on the electricity generation portfolio–a scandinavian-german case study," *Applied Energy*, vol. 235, pp. 1637–1650, 2019.

[59] F. M. Andersen, H. K. Jacobsen, and P. A. Gunkel, "Hourly charging profiles for electric vehicles and their effect on the aggregated consumption profile in denmark," *International Journal of Electrical Power & Energy Systems*, vol. 130, p. 106900, 2021.

[60] Q. Wang, X. Liu, J. Du, and F. Kong, "Smart charging for electric vehicles: A survey from the algorithmic perspective," *IEEE Communications Surveys & Tutorials*, vol. 18, no. 2, pp. 1500–1517, 2016.

[61] K. Maeng and Y. Cho, "Who will want to use shared autonomous vehicle service and how much? a consumer experiment in south korea," *Travel Behaviour and Society*, vol. 26, pp. 9–17, 2022.

[62] B. Ma, D. Hu, Y. Wang, Q. Sun, L. He, and X. Chen, "Time-dependent vehicle routing problem with departure time and speed optimization for shared autonomous electric vehicle service," *Applied Mathematical Modelling*, vol. 113, pp. 333–357, 2023.

[63] M. Saleh, A. Milovanoff, I. Daniel Posen, H. L. MacLean, and M. Hatzopoulou, "Energy and greenhouse gas implications of shared automated electric vehicles," *Transportation Research Part D: Transport and Environment*, vol. 105, p. 103233, 2022.

Appendix A

Single line diagrams of N44 and N46

Figure A.1: Single line diagram of the original network model Nordic 44.

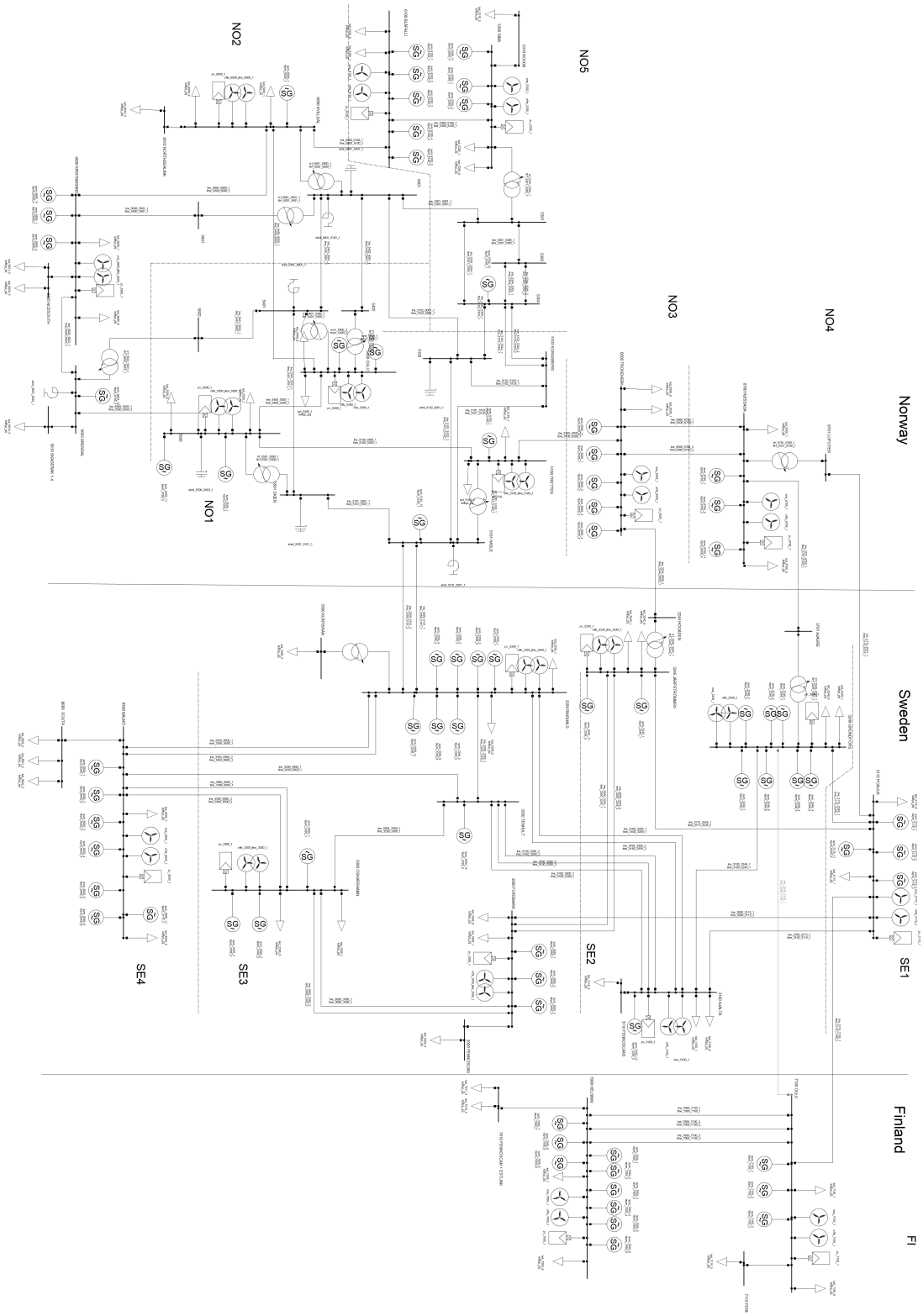

Figure A.2: Single line diagram of the updated network model Nordic 46. Note that the line between nodes 2349 Grundfors in SE2 and 7100 Oulu in FI has been disconnected and is out of service, since no such line exists in reality or in Svk's data.